Case Studies in Construction Materials 18 (2023) e02171

Contents lists available at ScienceDirect

Case Studies in Construction Materials

journal homepage: www.elsevier.com/locate/cscm

Post-fire behaviour of concrete containing nano-materials as a cement replacement material

Balamurali Kanagaraj [a], N. Anand [a,*], Katherine A. Cashell [b,*], A.Diana Andrushia [c]

[a] Department of Civil Engineering, Karunya Institute of Technology and Sciences, Coimbatore, India
[b] Department of Civil, Environmental, and Geomatic Engineering, University College London, London, United Kingdom
[c] Department of Electronics and Communication Engineering, Karunya Institute of Technology and Sciences, Coimbatore, India

ARTICLE INFO

Keywords:
Nanomaterials
Concrete
Durability
Elevated temperature
Post-fire

ABSTRACT

Cement replacement materials have been the subject of increasing levels of research and development in recent years. These products are employed for many reasons, including to modify the properties of concrete, although the most urgent need for their use currently is to produce more sustainable concrete and reduce waste. Recently, nanomaterials such as nano-fly ash and nano-metakaolin have been studied as cement replacement materials as they tend to fill the pores present in the matrix, thereby increasing the density of the concrete resulting in an enhanced hydration process and greater mechanical performance. This paper is concerned with the post-fire mechanical and durability behaviour of concrete containing nanomaterials as a cement replacement material, for which there is no information available currently. The key information and results from an experimental investigation are presented and discussed. The experimental programme studied both nano-fly ash and nano-metakaolin with a cement replacement ratio of between 5% and 25%. The specimens were subjected to a standard fire and then cooled either slowly, in air, or quickly in water. Based on the test data, it is concluded that the presence of either of these nanomaterials in concrete reduces the pore volume and increases the pozzolanic activities in the mix, leading to enhanced mechanical and durability behaviour compared with traditional concrete. The optimization trials indicate that the best replacement ratios are 20% for the nano-fly ash and 15% for the nano-metakaolin. Overall, following elevated temperature exposure, the concretes containing nano-fly ash performed better than the concretes with nano-metakaolin but both out-performed traditional cement-based concrete.

1. Introduction

This paper is concerned with the behaviour of concrete comprising nano-materials as a cement-replacement product, following exposure to elevated temperature. In recent decades, the global consumption of construction materials has created a reduction in availability of virgin raw materials, including cement. Many engineers and researchers have proposed and studied alternatives to cement in concrete mixes, and these are increasingly expected to not only improve the material behaviour but also to enhance the sustainability of construction [1]. Early cement-replacement products included the industrial by-product fly ash, silica fume and

* Corresponding authors.
E-mail addresses: balamuralik20@karunya.edu.in (B. Kanagaraj), nanand@karunya.edu (N. Anand), k.cashell@ucl.ac.uk (K.A. Cashell), diana@karunya.edu (A.Diana Andrushia).

https://doi.org/10.1016/j.cscm.2023.e02171
Received 17 March 2023; Received in revised form 16 May 2023; Accepted 27 May 2023
Available online 7 June 2023

metakaolin. These are pozzolanic materials and therefore can be used as binders in concrete production, in place of cement. All of these cement-replacement products enhance the strength of concrete compared with traditional cement and offer further advantages for both fresh and hardened concrete such as resistance to chloride penetration. However, they each also come with their own unique characteristics which can be influential to the concrete performance. For example, using silica fume generally requires the addition of superplasticizers to the mix to enhance the fresh properties [2]. Concrete which includes metakaolin tends to exhibit superior strength and sorptivity properties compared to fly ash-blended concrete or mixes with no supplementary cementitious materials [3]. Moreover, metakaolin-blended concrete has greater resistance to water penetration through capillary action, compared with conventional concrete [4]. The optimum dosage of fly ash, metakaolin and silica fume in cement composites has been found to be between 15% and 25%, 5–15% and 5–10%, respectively [5].

The use of nanomaterials in the construction sector is an emerging field of study and research [6]. When used in concrete mix designs, the nanomaterials fill the micro-pores present in the matrix, thereby reducing the porosity of the mix and increasing the bond between the aggregates and thereby enhancing the strength and durability of the concrete [7]. It has been verified using a scanning electron microscope (SEM) that incorporating nanomaterials in concrete results in a denser paste compared with cement-based mixes [8]. The use of nanomaterials also increases the corrosion resistance, determined using the permeability test and the chloride penetration test [9], and reduces the sorptivity and chloride permeability. The age-effect on the mechanical properties of concrete with various dosages of two different nanomaterials, namely nano-silica (NS) and nano-clay (NC), was studied and it was shown that including nanomaterials improves the hardened concrete properties of the mix. The concrete with NS exhibited superior performance compared with NC in terms of the mechanical properties due to its dense microstructure [10].

After exposure to high temperatures, above 300 ℃, the residual compressive strength of cementitious materials tends to decrease. However, the addition of 1% of nanoparticles to such materials can maintain higher residual compressive strengths (10–20% higher) following exposure of up to 700 ℃ [11–14]. Lower permeability can also be achieved when higher percentages of nanoparticles are added, which is beneficial for high-strength concrete (HSC). However, as previously discussed, this can have a detrimental effect when the materials are exposed to high temperatures. Nevertheless, when the water-to-cement ratio increases, the optimum replacement ratio of nanoparticles can increase by up to 3%, despite the lower strength of the cement-based compositions [7].

The addition of superplasticizer can also have a positive effect on the residual properties, which are usually higher than at ambient temperatures [15]. Adding 1% of nano-alumina can improve the elastic modulus of such mixtures following exposure to elevated temperatures of up to 400 ℃. However, this can cause the concrete to become stiffer but more brittle [11]. On the other hand, to achieve the highest residual strength of cementitious mortars with the introduction of nano-titania particles, 2% of such nanoparticles are required [14]. Moreover, the combined addition of micro-silica and nano-silica particles has more substantial synergistic effects on the residual compressive strength of cement-based mortars when their contents are similar [12]. In the case of employing nano-iron oxide Fe_2O_3, NF, it is recommended that this type of nanoparticle be produced by thermal decomposition of basic ferric acetate calcined at 275 ℃, as this provides better results in terms of the residual strength of respective mortars [16]. In contrast, the effect of zinc oxide nanoparticles has been shown to be almost negligible following exposure to high temperatures [17].

Partially replacing Portland cementitious plasters with nano-metakaolin and fly ash has been found to have a significant impact on their residual properties following exposure to elevated temperature. For instance, when mortar mixes were designed with a cement replacement ratio of 10% of nano-metakaolin and 10% nano-fly ash, the reduction in the residual compressive strength was only 16.67% following exposure to 800 ℃ (the compressive strength reduced from 36 to 30 MPa), whereas a mix with 100% ordinary Portland cement experienced a corresponding reduction of 83% (with the compressive strength reducing from 30 to 5 MPa) [18]. It is worth noting that nano-metakaolin is produced from kaolinite clay through the calcination process, which results in a thermally activated alumino-silicate at 800 ℃ [19]. This characteristic makes the mortars stronger and more fire-resistant.

A study conducted by Arash et al. [20] investigated the effects of incorporating multi-walled carbon nanotubes (MWCNTs) into cement bricks exposed to elevated temperatures. The cement bricks were made with admixtures containing 0.02, 0.05, 0.1, and 0.2 wt % of MWCNT and were subjected to temperatures of 300, 600, and 800 °C. The results indicated that the samples exposed to 300 °C, with 0.1 wt% of MWCNT, demonstrated a 41% improvement to the residual compressive strength compared to a plain concrete control sample. However, following exposure to higher temperatures (600 and 800 °C), the samples showed similar relative residual strength compared with the plain concrete samples. Furthermore, the study suggested that MWCNTs could serve as bridges between hydrates and cracks, which could improve the stability of composite structures, even at temperatures as high as 800 °C [21].

Nano-Fe_3O_4 and nano-Fe_2O_3 are additional nanoscale materials that have been used to enhance the thermal resistance of cement. In a study conducted by Hwang et al. [22], the effects of nano iron oxide admixtures (up to 3 wt%) on the thermal resistance of cement pastes were evaluated after being exposed to temperatures ranging from 10 °C to 800 °C. The results indicated that even small amounts of nanoparticles (1% by weight of cement) improved the thermal resistance of the samples, while maintaining the compressive strength, reducing the mass loss, and decreasing the porosity. Abdalla et al. [23] examined the impact of nano-Fe_2O_3 admixtures, ranging from 1 to 3 wt%, on the properties of cement pastes subjected to high temperatures (200–1000 °C), and found that the presence of nano-Fe_2O_3 particles was particularly effective in reducing the length of cracks in cement pastes.

The incorporation of nano-titania particles into cement-based composites exposed to high-temperature conditions has attracted growing attention from researchers. In a study by Selim et al. [24], the effects of adding nano-titania (up to 1 wt%) into high-alumina, low-cement refractory castable heated to very high temperatures of 1250 °C were evaluated. The findings indicated that the addition of titania (particularly at 0.5 wt%) led to a reduction in the apparent porosity of the material, while increased the crushing strength and modulus of rupture of the samples. However, the authors also noted that excessively high amounts of nano-titania could result in decreased final castable properties after heating. Farzadnia et al. [25] examined the effects of nano-titania as a cement replacement (at 1, 2, and 3 wt%) on the thermal resistance of cement mortars exposed to high temperatures (up to 1000 °C). The results indicated that

an optimal amount of nano-titania (i.e., 2 wt%) improved the residual compressive strength of mortars following exposure of up to 400 °C. Additionally, a slight reduction in the permeability of mortars modified with nano-titania (when exposed to temperatures up to 300 °C) was observed.

The enhancement of thermal resistance in cement-based composites is often achieved by incorporating nano-sized admixtures. Among these, nano-silica is the most widely used due to its pozzolanic activity and pore-filling properties that refine the microstructure of cementitious materials [26,27]. Khater et al. [28] investigated the effect of adding 5% nano-silica on the thermal resistance of cement pastes exposed to high temperatures. The study revealed a significant improvement in the thermal resistance of cement pastes containing 5% nano-silica as compared to the control sample with 100% cement. This improvement was attributed to the enhancement of the C-S-H phase in the cement paste.

Nano-silica is a popular admixture for improving the thermal resistance of cementitious composites due to its pozzolanic activity and pore-filling effect, which refine the microstructures [29,30]. The study conducted by Khater et al. [28] evaluated the effects of adding 5% nano-silica to cement pastes exposed to elevated temperatures and showed a noticeable improvement in the thermal resistance due to the improvement of the C-S-H phase. Heikal [31] also observed an improvement in thermal resistance in cement pastes containing ground granulated blast-furnace slag (GGBFS) and nano-silica (up to 4 wt%), which exhibited higher compressive strength than control samples. Similarly, Norhasri et al. [6] found that nano-silica contributed to an increase in residual compressive strength in high-volume fly ash mortars following exposure to elevated temperatures, and this was attributed to the nano-filling effect and the greater extent of the C-S-H phase produced. In a study by Kanagaraj et al. [15], nano-silica was found to be more effective than silica fume (SF) in improving the mechanical properties of high-strength concretes, with higher values of residual compressive strength and greater prevention of crack propagation.

The current paper is concerned with the post-fire behaviour of concrete with nanomaterials. When any concrete is exposed to elevated temperature, as occurs during a fire, the mechanical properties such as strength and stiffness degrade with increasing temperature. Generally, concrete can retain a sufficient degree of its strength up to around 500℃ but after this it loses strength rapidly due to the development of micro-cracks, increased pore pressure, and spalling [32,33]. Less porous concrete is more susceptible to strength loss at elevated temperature due to the high thermal incompatibility and internal pressure which develops in the matrix. These factors cause a discontinuity between the binder and filler materials [34], which can lead to excessive cracking [35] and explosive spalling [36]. High-strength concrete is more susceptible to spalling due to the formation of greater pore pressure, compared with normal strength grades [37]. It was shown that high-strength concrete blended with metakaolin loses significant strength when exposed to temperatures in excess of 800 ℃ [38]. The effect of temperature exposure on concrete made with NS and nano-ground granulated blast furnace slag (NG) was examined and it was shown that the NS-based mix lost a greater proportion of its strength during exposure to elevated temperature, compared with NG-based composites [39]. These studies show that the ingredients used in the concrete mix design are very influential to the elevated temperature performance, although this is not always considered in design.

In terms of the post-fire behaviour, which is the focus in the current paper, when concrete is cooled following exposure to elevated temperatures, it generally regains some of the strength lost during the fire. Specimens which are cooled relatively quickly, such as by cold water, tend to lose a greater proportion of the original strength, compared with specimens which are allowed to cool at a slower rate, such as naturally in air [40]. This is owing to the thermal shock which occurs at the surface of the specimens [41]. To date, studies into the post-fire behaviour, including the phase changes and thermal response, of nanomaterial-blended cement composites are very scarce.

In this context, the objectives of the current paper are to present the details, results and analysis from a series of tests to determine the properties of different concrete mixes containing either nano-fly ash (hereafter referred to as NF) or nano-metakaolin (NM) in place of cement, following exposure to different levels of elevated temperature and then cooled either quickly, in water, or slowly, in air. The nanomaterials are included in the design mixes in various proportions ranging from 5% to 25%. After curing for 28 days, the NF- and NM-blended concretes were exposed to different levels of elevated temperature, representing either 30, 60, 90 or 120 min of fire exposure in accordance with an ISO 834 standard fire, and then cooled. The specimens were then examined to determine their post-fire mechanical and durability performance. The paper proceeds with an overview of the test programme, including the specimen designs and test methodology, and this is followed by a detailed analysis of the results.

2. Test materials and methodology

2.1. Concrete materials

The concrete employed in this study included ordinary Portland cement (OPC), manufactured sand as the fine aggregate, locally-sourced crushed granite as the coarse aggregate (CA) as well as NF and NM as the nanomaterials, to replace different proportions of the OPC. Grade 53 OPC, in accordance with IS 12269 [42] was employed as the primary binder material and this had a specific gravity

Table 1
Physical properties of the NF and NM nanomaterials.

	NF	NM
Specific gravity (SG)	2.13	2.5
Specific surface area (m^2/g)	500–900	15000–18000
Colour	Blackish grey	Ivory to Cream

(SG) of 3.13. The manufactured sand had a SG and fineness modulus of 2.7 and 2.56, respectively, and were therefore classified as zone II in accordance with IS 383 [43]. The crushed granite aggregate had a SG of 2.76. Different quantities of NF and NM were employed in the concrete mixes as a replacement for OPC in proportions between 5% and 25%, in 5% increments, for the NF-blended concretes and 5% and 20% for the NM-mixed composites. The physical properties of the NF and NM employed in this study, are presented in Table 1. In addition, the oxide composition of both is given in Table 2.

2.2. Specimen preparation

2.2.1. Mix design

The test specimens were made using grade M30 concrete and the binder, filler and water content of the mix were in accordance with the guidance given in IS 10262 [5]. The mix designs for all of the concretes examined in this programme are presented in Table 3, including the amount of nanomaterials included in each mix (in kg/m^3), and the quantities of cement, fine aggregates (FA) and course aggregates (CA) included in each case. The mix name indicates the type of nanomaterial employed in the concrete, as well as the cement replacement ratio (between 5% and 25% for NF and 5% and 20% for NM). The table also includes the water to cement (w/c) ratio. A control case mix was also designed (given as CC in Table 3), which contained no nanomaterials, for comparison.

2.2.2. Casting and curing

The concrete was mixed using a rotary-type mixer, using the following protocol: (i) first, the dry course and fine aggregates were mixed in the mixer drum for 1–2 min; (ii) then, the binder materials (i.e. cement and nanomaterials, if used) were added and allowed to rotate in the mixer drum for another 2–3 min to obtain uniformity in mixing; and finally, (iii) after achieving uniformity, the universal solvent (water) was added to the mix, and the mix was allowed to rotate in the mixer drum to achieve uniform consistency [44]. Once these steps were complete, the workability of the freshly prepared concrete was examined using a slump cone test in accordance with the guidelines given in ASTM C 143 [45]. A combination of cubic specimens (150 mm × 150 mm × 150 mm), cylindrical samples (either 300 mm in height with a cross-sectional diameter of 150 mm or 100 mm in height with a cross-sectional diameter of 50 mm), and beams (500 mm in length with a square cross-section of 100 mm × 100 mm) were cast and then transferred to a vibrating table to ensure proper compaction. The specimens were kept in air, at room temperature, for the first 24 h after casting in order to initiate the heat of hydration and setting of the concrete. After setting, the test specimens were cured in a curing tank for a period of 28 days or until the day of testing.

2.2.3. Heating and cooling procedure

An electric furnace of size 700 × 400 × 400 mm was used to heat the concrete specimens to a target temperature of either 821 ℃, 925 ℃, 986 ℃ or 1029 ℃, representing an ISO 834 standard fire after 30, 60, 90 or 120 min, respectively. The temperature in the furnace, and in the concrete specimens, was measured using K-type thermocouples as indicated in Fig. 1. Once the target temperature was reached, the furnace was turned off, and some of the specimens were allowed to cool naturally in air (hereafter referred to as AC). On the other hand, the rest of the specimens were cooled using water (WC).

2.3. Test methodologies

A number of different tests were conducted on each specimen, after cooling, in order to determine the post-fire properties of concrete with various amounts of nanomaterials, as cement-replacements, in the design mix. For all of the tests described hereafter, three repeats were conducted for each mix and the average is taken as the result presented in the paper. The following sub-sections describe these tests.

2.3.1. Hardened concrete properties

2.3.1.1. Change in mass. All of the concrete specimens were carefully weighed before heating (w_1), and again after the heating/cooling procedure (w_2) and Eq. (1) was used to obtain the change in mass (L), as a percentage, of the concrete composite after temperature exposure:

Table 2
Oxide composition of the NF and NM nanomaterials.

Constituents (%)	NF	NM
SiO_2	59.9	58.55
Fe_2O_3	1.28	3.44
Al_2O_3	32.29	28.2
CaO	0.04	2.23
MgO	0.17	0.32
Na_2O	0.24	0.58
K_2O	2.83	1.26
SO_3	—	0.07

Table 3
Mix designs for grade M30 concrete with different cement replacement ratios.

Mix name	Cement (OPC) (kg/m^3)	FA (kg/m^3)	CA (kg/m^3)	Nano-powder		w/c ratio
				NF (kg/m^3)	NM (kg/m^3)	
CC	372	607	1214	-	-	0.45
NF5	353.4	607	1214	18.6	-	0.45
NF10	334.8	607	1214	37.2	-	0.48
NF15	316.2	607	1214	55.8	-	0.52
NF20	297.6	607	1214	74.4	-	0.56
NF25	279	607	1214	93	-	0.60
NF30	260.4	607	1214	111.6	-	0.60
NM5	353.4	607	1214	-	18.6	0.50
NM10	334.8	607	1214	-	37.2	0.54
NM15	316.2	607	1214	-	55.8	0.58
NM20	297.6	607	1214	-	74.4	0.58

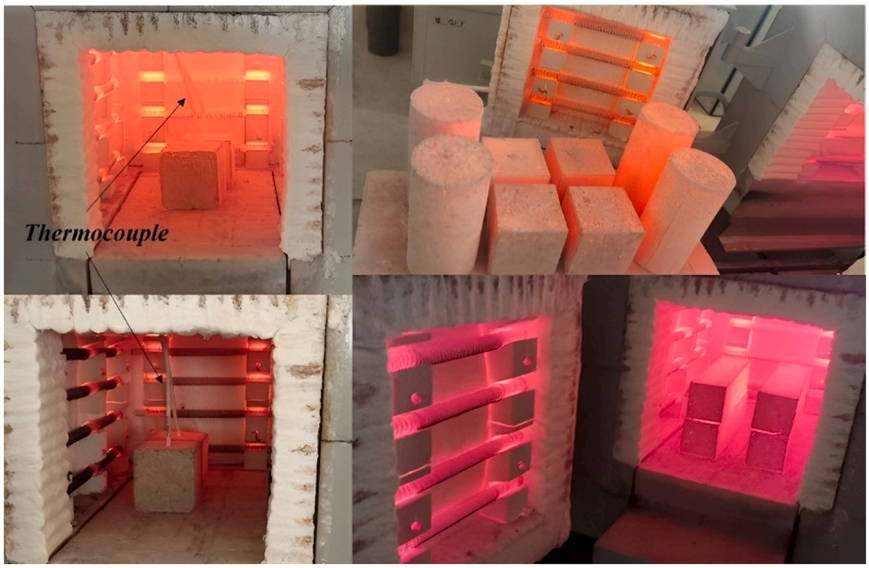

Fig. 1. Heating of concrete samples in the furnace.

$$L = \frac{w_1 - w_2}{w_1} \times 100 \quad (1)$$

2.3.1.2. Ultrasonic pulse velocity (UPV) test. An ultrasonic pulse velocity (UPV) test is a non-destructive test typically used to check the quality of hardened concrete, and also to detect defects or the presence of voids and discontinuities in the material. It is conducted by passing an ultrasonic pulse through the concrete, and the velocity of the pulse which passes through is related to the mechanical properties. Relatively high velocities indicate good quality of the material, and therefore good mechanical properties, whereas slower velocities suggest concrete with defects or voids. In this programme, a UPV test was conducted on 150 × 150 × 150 mm^3 cubic specimens and the tests were completed in accordance with the guidance given in IS 13311 [46].

2.3.1.3. Compressive strength test. A compressive strength test was conducted on 150 × 150 × 150 mm^3 cubic specimens to examine the ultimate strength of the mix in accordance with IS 516 [47]. A computerized compression testing machine with a maximum capacity of 2000 kN was employed and a loading rate of 0.25 MPa/s was applied until failure occurred by crushing. This test was conducted on samples before heating, and also following the heating/cooling procedure.

2.3.1.4. Splitting tensile strength test. The tensile strength of the concrete was determined by conducting a splitting test on 300 mm × 150 mm cylindrical samples before and after temperature exposure; the tests were completed in accordance with IS 5816 [48]. The loading rate in the tests was between 0.7 and 1.4 Pa/s which was applied to the cylinder specimens until failure occurred.

2.3.1.5. Flexural strength test. The flexural strength test was performed using 500 × 100 × 100 mm prism specimens, in accordance with IS 516 [47]. A universal testing machine with a capacity of 1000 kN was employed for these tests, and the loading rate was

0.886–1.21 MPa/min until failure occurred.

Table 4 summarises all the above-mentioned mechanical tests on hardened concrete in the current programme, both before and following exposure to elevated temperature.

2.3.2. Durability properties

2.3.2.1. Water permeability. The water permeability test for concrete was conducted in accordance with IS 3085 [49]. The aim was to determine the water permeability coefficient K both before and after temperature exposure, in accordance with Eq. (2):

$$K = \frac{Q}{A \times T \times \frac{H}{L}} \tag{2}$$

where Q is the water quantity in millilitres percolating through the test sample during the test, A is the cross-sectional area of the test sample, in cm^2, T is the time in seconds, H is the pressure head (in m) and L is the sample thickness (in the same unit as H, so m in this case). These tests were conducted on cylindrical samples which were 100 mm in length and had a cross-sectional diameter of 50 mm.

2.3.2.2. Rapid chloride penetration test. The rapid chloride penetration tests were conducted in accordance with ASTM C 1202–19 [50], and the aim was to determine the resistance of the various concrete mixes to chloride ion penetration both before and after elevated temperature exposure. In this test, a constant voltage V equal to 60 V was applied to cylindrical specimens with a height of 100 mm and cross-sectional diameter of 50 mm, for a period of 6 h. During the test, the sample was placed between two reservoirs, one of which contained NaCl with a concentration of 30 g/litre, and the another which contained a NaOH solution with a concentration of 12 g/litre. The reservoirs were connected to a DC power supply and a current was passed through the concrete sample was measured to determine the permeability. A relatively high current value implies a more permeable concrete compared with a lower value.

2.3.3. Microstructural properties

In order to determine any changes to the microstructure of the concrete mixes following exposure to elevated temperature followed by cooling, a series of images were taken both before and after heating using a scanning electron microscope (SEM). The images obtained from the SEM are useful for visualizing the microstructure of the hydrated cement paste, which relates to the concrete strength and durability. This analysis was conducted for the control concrete (CC) as well as the concrete mixes with 20% cement replacement ratio using NF and 15% cement replacement ratio using NM nanomaterials. These were selected following an analysis of the mechanical and durability properties of all the mixes in the current study, as discussed later in this paper.

3. Results and discussion

In this section, the results from the aforementioned tests on concretes with varying levels of nanomaterials included in the concrete mix, and following exposure to different levels of elevated temperature, are discussed. The influence of nanomaterial type, replacement ratio, fire exposure time and cooling rate on the residual mechanical properties are analysed in detail. It is noteworthy that in the presented results graphs, the results for NF-blended concretes are presented first, followed by the corresponding results for NM-blended concretes, and a consistent formatting approach is adopted throughout for ease of comparison and visualisation. Therefore, solid lines in the graphs refer to air-cooled specimens whilst dashed lines are for water-cooled samples. Identical colours are used for samples with similar nanomaterial replacement ratios.

3.1. Change in mass

The change in mass of the concrete after exposure to elevated temperature is depicted in Figs. 2 and 3 for mixes with NF and NM nanomaterials, respectively. From the data presented, it is clear that an increase in temperature exposure time results in more significant mass loss in the concrete specimens. For specimens exposed to 30 min of heating, the mass loss was relatively minor, and there

Table 4
Details of test specimens for examination of the properties of hardened concrete.

Type of Nanomaterial	Replacement ratio of concrete with nanomaterials (%)	Type of Specimen	Exposure Condition	Cooling method
Compressive strength tests				
NF	5, 10, 15, 20, 25	150 × 150 × 150 mm^3 cubes	Reference	-
NM	5, 10, 15, 20		Heated	Air/Water
Tensile strength tests				
NF	5, 10,15, 20, 25	150 mm × 300 mm cylinders	Reference	-
NM	5, 10, 15, 20		Heated	Air/Water
Flexural strength tests				
NF	5, 10, 15, 20, 25	500 mm (length)	Reference	-
NM	5, 10, 15, 20	× 100 mm × 100 mm	Heated	Air/Water

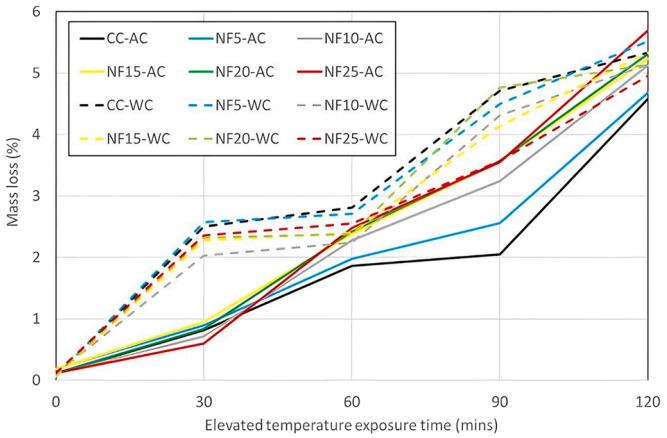

Fig. 2. Mass loss of NF-blended specimens following exposure to a standard fire and subsequent cooling in air (AC) or water (WC).

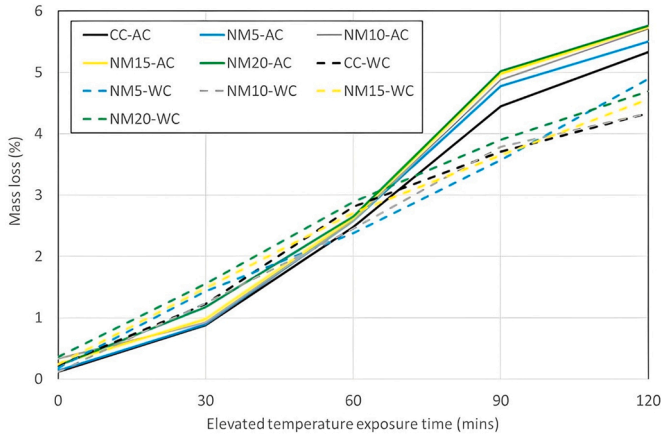

Fig. 3. Mass loss of NM-blended specimens following exposure to a standard fire and subsequent cooling in air (AC) or water (WC).

was a slight increase in strength also observed; this is likely to be due to the acceleration of the rate of hydration of the calcium silicate hydrate (CSH) gel. When the temperature duration increased from 30 to 60 min, the mass loss became more evident owing to the evaporation of capillary water both for the air-cooled (AC) and water-cooled (WC) samples. Even for the samples with a relatively

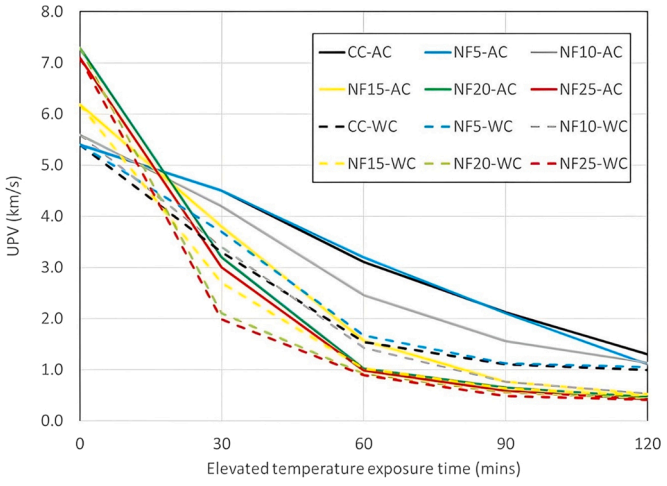

Fig. 4. Ultrasonic pulse velocity for NF-blended specimens after exposure to elevated temperature and subsequent cooling.

greater proportion of nanoparticles in the mix, the total reduction in mass was greater when the concrete was exposure to higher temperatures. In general, the samples that were cooled faster by water cooling, experienced greater mass loss compared with the air-cooled samples. From the data presented in Figs. 2 and 3, it is clear that the NM-blended concrete samples experienced greater mass losses compared with the NF-blended mixes. When the heating duration increased to either 90 or 120 min of standard fire exposure, the chemically bound water in the CSH gel started to dehydrate and thus further reduced the mass of the samples.

3.2. Concrete quality by UPV test

In these tests, an electronic pulse was passed through concrete cubes to determine the quality of the hardened material and to detect the level of defects that were present. Figs. 4 and 5 present the test results in terms of velocity of the pulse transmitted (in km/s) for each of the concrete mixes containing different proportions of NF and NM nanoparticles, respectively, following exposure to elevated temperature and cooling either in air (AC) or water (WC). The corresponding concrete qualities, deduced from the velocities measured in the tests in accordance with the guidance given in IS 13311 Part1 [46], are presented in Tables 5 and 6. In these tables, the concrete quality is graded as being either excellent (E), good (G), moderate (M) or doubtful (D), based on the UPV test results.

It is clear that the samples which were exposed to greater temperatures, and therefore longer fires, experienced a greater reduction in velocity during the UPV test compared with those exposed to shorter fires. The reduction in UPV which occurred for the longer-heated specimens was due to the formation of cracks in the concrete, which lead to discontinuities between the binder and filler materials. This then had a consequent effect on the quality of concrete, as given in Tables 5 and 6. It is clear from these tables that all concretes were of doubtful quality following exposure to 90 min or more of elevated temperature. For the NF-blended samples, after 60 min of fire exposure and subsequent cooling, all but one sample (NF5-AC) were also classified as doubtful quality. Generally, the post-fire quality was marginally better for the NM-blended samples compared with the NF-containing concretes on a like-for-like basis. The UPV of the specimens which were cooled in water was lower than for the specimens cooled in air; this is attributed to the formation of a large number of cracks during the quenching process. Specimens exposed to elevated temperature and cooled in water exhibited doubtful quality.

3.3. Compressive strength

The residual compressive strengths of the various concrete composites, exposed to heating and cooling, are presented in Figs. 6 and 7 for samples with NF and NM materials included in the design mix, respectively. In addition, Tables 7 and 8 present the corresponding numerical values, together with the mean, standard deviation (SD) and coefficient of variation (COV) for each set of testing conditions. At ambient temperature, samples NF-20 and NM-15 had the greatest initial compressive strengths of the concretes made with NF and NM nanomaterials, respectively. These samples remained the strongest, for each of the different elevated temperature exposure durations. It is noteworthy that the concrete blended with NF nanomaterials retained almost all of their original strength even after 30 min of elevated temperature exposure. All of the concretes examined in this programme lost a notable proportion of their original compressive strength following exposure to elevated temperature for 60 min or more. This is due to the physical and chemical changes which occur during the hydrated phases.

When the control case (CC) was exposed to a temperature of 925 ℃ for 60 min, it experienced losses of compressive strength of 17.3% and 14.6% for the air- and water-cooled conditions, respectively. This reduction in strength is attributed to the evaporation of chemically-bound water, which leads to the transformation of CSH to CaO in the composite, causing a degradation in the chemical bonding between the binder and filler materials and reduced compressive strength. In comparison, the NF-20 and NM-15 mixes also

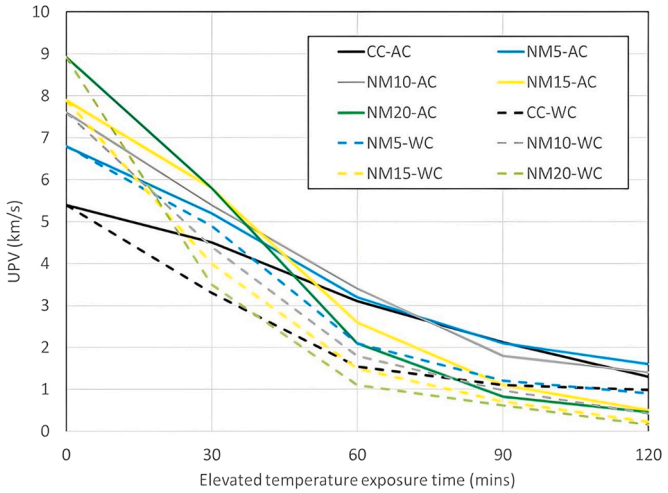

Fig. 5. Ultrasonic pulse velocity for NM-blended specimens after exposure to elevated temperature and subsequent cooling.

Table 5
Post-fire quality of NF-blended concrete in accordance with IS 13311 [46].

Sample	30 min		60 min		90 min		120 min	
	AC	WC	AC	WC	AC	WC	AC	WC
NF5	E	G	M	D	D	D	D	D
NF10	G	M	D	D	D	D	D	D
NF15	G	D	D	D	D	D	D	D
NF20	M	D	D	D	D	D	D	D
NF25	M	D	D	D	D	D	D	D

Key: E– Excellent; G– Good; M – Moderate; D – Doubtful

Table 6
Post-fire quality of NM-blended concrete in accordance with IS 13311 [46].

Sample	30 min		60 min		90 min		120 min	
	AC	WC	AC	WC	AC	WC	AC	WC
NM5	E	E	G	D	D	D	D	D
NM10	E	G	M	D	D	D	D	D
NM15	E	G	D	D	D	D	D	D
NM20	E	M	D	D	D	D	D	D

Key: E– Excellent; G– Good; M – Moderate; D – Doubtful

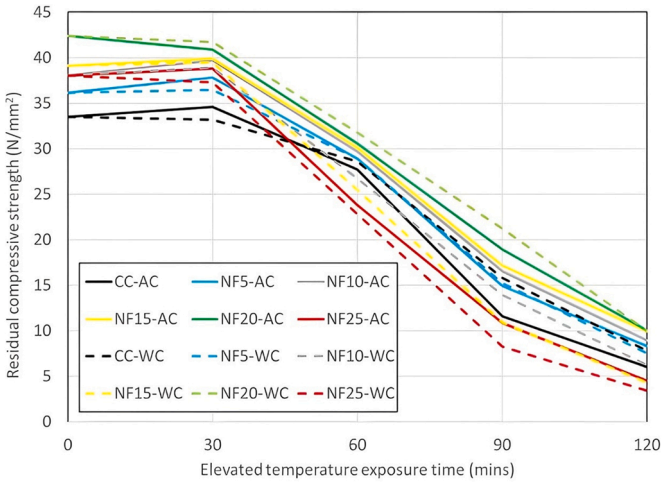

Fig. 6. Residual compressive strength of NF-blended concrete exposed to elevated temperature and then cooling.

experienced significant reductions in compressive strength when subjected to the same temperature and duration. The NF-20 mix lost 27.8% and 25% of its initial compressive strength for air-cooled and water-cooled conditions, respectively. The NM-15 mix experienced even greater loss of strength, with reductions of 53.9% and 52.7% for air-cooled and water-cooled conditions, respectively.

The results suggest that the addition of nanomaterials did not provide significant improvements to the resistance of concrete following exposure to high temperatures. This is likely due to the fact that the evaporation of chemically-bound water is the primary mechanism of strength loss in concrete under high-temperature conditions, and the addition of nanomaterials does not effectively prevent this process. Therefore, further research is needed to develop more effective methods to enhance the high-temperature resistance of concrete.

It is noteworthy that the concretes with the relatively high proportions of nanomaterials had the greatest compressive strength for all levels of temperature exposure. There was little notable difference between the strength retention of the concretes with NF versus those with NM, for the same replacement ratio. The samples that were cooled in water (WC) experienced a relatively greater loss in strength compared with the air-cooled (AC) specimens. This is attributed to the quenching effect whereby the relatively fast cooling process led to the formation of additional micro-cracks, resulting in greater strength loss. The dehydration of the CSH gel occurred at a temperature of approximately 400–450 ℃, which resulted in volume reduction in the concrete [51]. Also, there may have been decomposition of the CSH gel in the temperature range between 500 and 850 ℃ [52].

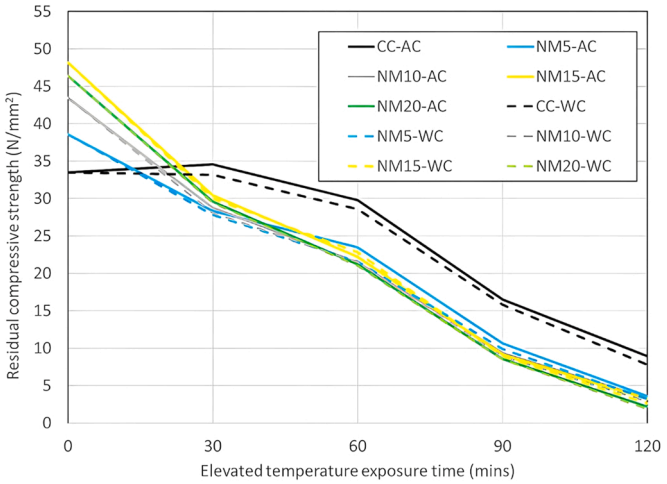

Fig. 7. Residual compressive strength of NM-blended concrete exposed to elevated temperature and then cooling.

Table 7
Compressive strength of the NF-blended concretes following exposure to various durations of elevated temperature.

Heating duration (mins)	**CC-AC**	**NF5-AC**	**NF10-AC**	**NF15-AC**	**NF20-AC**	**NF25-AC**
0	33.5	36.13	38.08	39.1	42.4	38
30	34.6	37.8	39.7	39.9	40.9	38.8
60	27.7	28.9	29.7	30.09	30.6	23.8
90	11.6	14.9	16.5	17.15	18.9	10.86
120	6	8.3	8.9	9.9	10	4.5
Mean	22.68	25.21	26.58	27.23	28.56	23.19
Standard deviation	13.09	13.07	13.49	13.34	14.02	15.53
COV (%)	0.58	0.52	0.51	0.49	0.49	0.67
Heating duration (mins)	**CC-WC**	**NF5-WC**	**NF10-WC**	**NF15-WC**	**NF20-WC**	**NF25-WC**
0	33.5	36.13	38.08	39.1	42.4	38
30	33.2	36.45	38.9	39.5	41.7	37.3
60	28.6	28.9	26.7	25.5	31.8	22.8
90	15.8	15.2	13.9	10.9	21.2	8.26
120	7.8	7.5	6.2	4.3	9.96	3.4
Mean	23.78	24.84	24.76	23.86	29.41	21.95
Standard deviation	11.46	12.96	14.52	16.05	13.89	16.01
COV (%)	0.48	0.52	0.59	0.67	0.47	0.73

Key: COV – Co-efficient of variation.

Table 8
Compressive strength of the NM-blended concretes following exposure to various durations of elevated temperature.

Heating duration (mins)	**CC-AC**	**NM5-AC**	**NM10-AC**	**NM15-AC**	**NM20-AC**
0	33.5	38.6	43.5	48.2	46.4
30	34.6	28.32	28.77	30.44	29.6
60	29.8	23.53	21.48	22.22	21.22
90	16.5	10.65	9.35	9.1	8.53
120	8.9	3.56	3.32	3.2	2.19
Mean	24.66	20.93	21.28	22.63	21.59
Standard deviation	11.38	13.97	15.93	17.86	17.51
COV (%)	0.46	0.67	0.75	0.79	0.81
Heating duration (mins)	**CC-WC**	**NM5-WC**	**NM10-WC**	**NM15-WC**	**NM20-WC**
0	33.5	38.6	43.5	48.2	46.4
30	33.2	27.8	28.11	30	29.4
60	28.6	21.6	21.55	22.77	21.01
90	15.8	9.91	8.88	8.91	8.46
120	7.8	3.22	2.88	2.66	1.89
Mean	23.78	20.23	20.98	22.51	21.43
Standard deviation	11.46	14.08	16.06	17.99	17.59
COV (%)	0.48	0.70	0.77	0.80	0.82

Key: COV – Co-efficient of variation.

3.4. Tensile strength

Figs. 8 and 9 depict the residual tensile strengths of concrete composites that were exposed to varying periods of heating and cooling, for the NF- and NM-blended mixes, respectively. The results indicate that the tensile strength of the concrete generally increased with higher proportions of nanomaterials in the mix, consistent with the observations on compressive strength at ambient temperature. The optimal replacement ratio for NF-blended concrete was found to be 20%, while it was 15% for the NM mixes.

All of the concrete mixes examined in the study exhibited some loss in strength following exposure to elevated temperatures for 30 min or more. The loss in tensile strength was slightly more significant for the NM-based mixes compared to the NF-based ones. This reduction in strength was attributed not only to the degradation of hydrated phases in the concrete but also to the thermal incompatibility between the binder and filler materials. Moreover, as observed in the previous section on compressive strength, the reduction in residual tensile strength was generally greater for specimens that were rapidly cooled by quenching in water compared to those that were air-cooled. The residual tensile strengths of the concrete composites exposed to different periods heating and cooling, are presented in Figs. 8 and 9 for the NF- and NM-blended mixes, respectively, and also in Tables 9 and 10, respectively.

3.5. Flexural strength

Figs. 10 and 11 illustrate the residual flexural strength of the NF- and NM-blended concrete mixes, respectively, following exposure to elevated temperatures and subsequent cooling. **The corresponding test data is presented in** Tables 11 and 12**, respectively.** As before with the compressive strength, the samples containing various proportions of NF in place of cement retained all of their original strength after exposure to 30 min of elevated temperature, and then cooling. After longer fires, the residual flexural strength decreased compared with the original values, as was also observed for the compressive and tensile strengths.

The effects of fire exposure on the flexural strength of concrete composites with varying replacement ratios of NM is depicted in Fig. 11. The results indicate that there was a slight reduction in flexural strength after 30 min of fire exposure, with more notable reductions observed after 60, 90, and 120 min of exposure. Similar to the observations for the compressive and tensile strengths, the optimal replacement ratios for NF and NM in the mix was found to be 20% and 15%, respectively. Higher replacement ratios led to greater losses in mechanical strength properties. The samples that were rapidly cooled in water exhibited greater residual flexural stiffness loss compared to those cooled slowly in air. This effect is clearly visible in Fig. 10, where all the dashed lines representing samples cooled in water reduced at a faster rate compared to the corresponding solid lines. In contrast, for the NM-blended concretes, this effect was less visible, although it is interesting to note that for these samples, the control case (CC) performed better in terms of post-fire residual flexural strength compared to the samples with nano-metakaolin included in the mix design.

3.6. Water permeability

In this experimental programme, the water permeability of the various concrete mixes following heating and cooling is assessed using two different test methods, previously introduced. These are the water permeability test and the rapid chlorine penetration test, and the results of both are discussed hereafter.

3.6.1. Water permeability test results

Tables 13 and 14 present the results from these tests in the form of the coefficient of water permeability (K) given in cm/sec. The results indicate that an increase in the relative content of NF and NM in the mix led to a reduction in the permeability of the concrete.

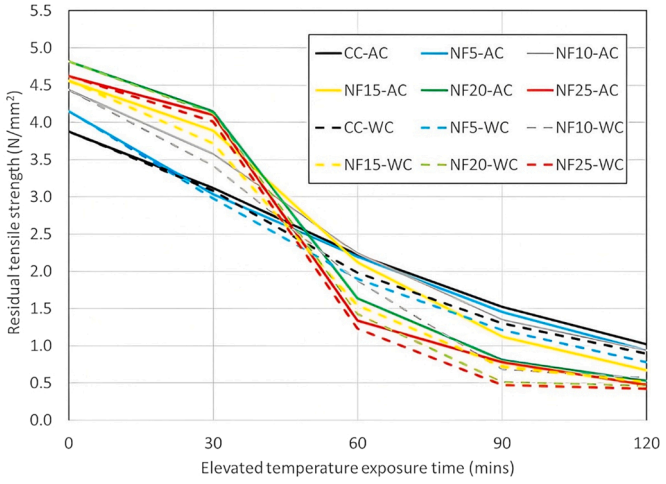

Fig. 8. Residual tensile strength of NF-blended concrete exposed to elevated temperature and then cooling.

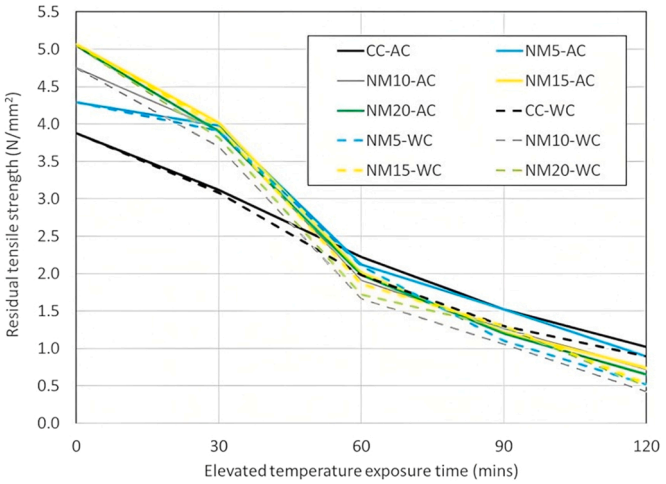

Fig. 9. Residual tensile strength of NM-blended concrete exposed to elevated temperature and then cooling.

Table 9
Tensile strength of the NF-blended concretes following exposure to various durations of elevated temperature.

Heating duration (mins)	CC-AC	NF5-AC	NF10-AC	NF15-AC	NF20-AC	NF25-AC
0	3.88	4.15	4.44	4.56	4.82	4.62
30	3.12	3.04	3.58	3.89	4.15	4.1
60	2.22	2.2	2.24	2.12	1.64	1.34
90	1.52	1.45	1.35	1.12	0.81	0.78
120	1.02	0.94	0.94	0.67	0.53	0.47
Mean	2.35	2.36	2.51	2.47	2.39	2.26
Standard deviation	1.16	1.28	1.48	1.70	1.97	1.95
COV (%)	0.49	0.54	0.59	0.69	0.82	0.86
Heating duration (mins)	**CC-WC**	**NF5-WC**	**NF10-WC**	**NF15-WC**	**NF20-WC**	**NF25-WC**
0	3.88	4.15	4.44	4.56	4.82	4.62
30	3.08	2.98	3.42	3.72	4.12	4.01
60	1.98	1.9	1.87	1.54	1.43	1.23
90	1.3	1.21	0.68	0.72	0.51	0.47
120	0.89	0.78	0.57	0.51	0.46	0.42
Mean	2.23	2.20	2.20	2.21	2.27	2.15
Standard deviation	1.24	1.37	1.70	1.83	2.06	2.01
COV (%)	0.56	0.62	0.77	0.83	0.91	0.94

Key: COV – Co-efficient of variation.

Table 10
Tensile strength of the NM-blended concretes following exposure to various durations of elevated temperature.

Heating duration (mins)	CC-AC	NM5-AC	NM10-AC	NM15-AC	NM20-AC
0	3.88	4.29	4.75	5.07	5.04
30	3.12	3.98	3.92	4.02	3.9
60	2.22	2.12	1.91	2.01	1.98
90	1.52	1.52	1.27	1.22	1.2
120	1.02	0.89	0.72	0.74	0.65
Mean	2.35	2.56	2.51	2.61	2.55
Standard deviation	1.16	1.51	1.74	1.86	1.86
COV (%)	0.49	0.59	0.69	0.71	0.73
Heating duration (mins)	**CC-WC**	**NM5-WC**	**NM10-WC**	**NM15-WC**	**NM20-WC**
0	3.88	4.29	4.75	5.07	5.04
30	3.08	3.91	3.7	3.96	3.82
60	1.98	2.1	1.66	1.86	1.72
90	1.3	1.1	1.06	1.3	1.28
120	0.89	0.52	0.42	0.53	0.49
Mean	2.23	2.38	2.32	2.54	2.47
Standard deviation	1.24	1.67	1.83	1.90	1.89
COV (%)	0.56	0.70	0.79	0.75	0.77

Key: COV – Co-efficient of variation.

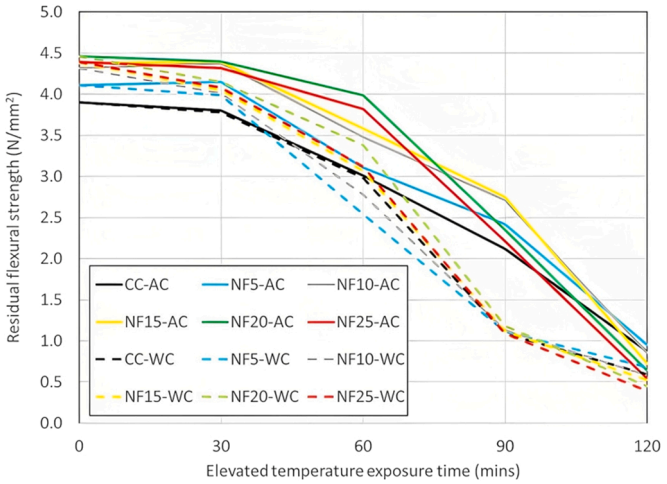

Fig. 10. Residual flexural strength of NF-blended concrete exposed to elevated temperature and then cooling.

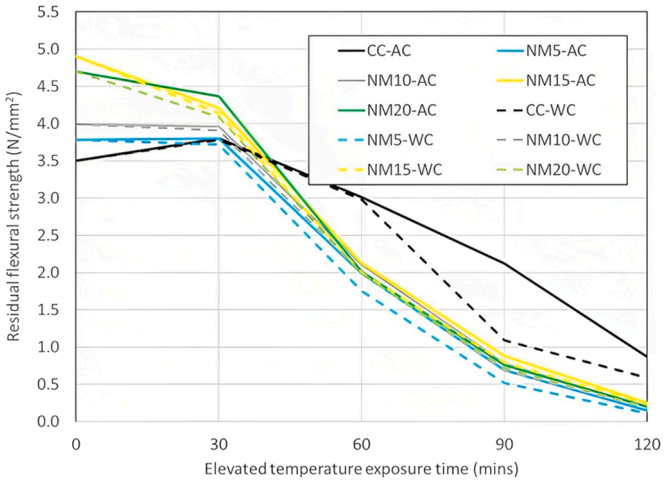

Fig. 11. Residual flexural strength of NM-blended concrete exposed to elevated temperature and then cooling.

Table 11
Flexural strength of the NF-blended concretes following exposure to various durations of elevated temperature.

Heating duration (mins)	**CC-AC**	**NF5-AC**	**NF10-AC**	**NF15-AC**	**NF20-AC**	**NF25-AC**
0	3.9	4.11	4.32	4.38	4.46	4.39
30	3.8	4.15	4.38	4.39	4.4	4.32
60	3.01	3.11	3.48	3.58	3.99	3.82
90	2.12	2.42	2.71	2.75	2.35	2.21
120	0.87	0.95	0.85	0.72	0.64	0.54
Mean	2.74	2.95	3.15	3.16	3.17	3.06
Standard deviation	1.27	1.33	1.46	1.52	1.65	1.66
COV (%)	0.46	0.45	0.46	0.48	0.52	0.54
Heating duration (mins)	**CC-WC**	**NF5-WC**	**NF10-WC**	**NF15-WC**	**NF20-WC**	**NF25-WC**
0	3.9	4.11	4.32	4.38	4.46	4.39
30	3.78	3.99	4.01	4.05	4.15	4.08
60	2.98	2.54	2.78	3.07	3.38	3.12
90	1.09	1.11	1.13	1.12	1.18	1.09
120	0.59	0.68	0.58	0.52	0.45	0.39
Mean	2.47	2.49	2.56	2.63	2.72	2.61
Standard deviation	1.54	1.59	1.67	1.73	1.81	1.79
COV (%)	0.62	0.64	0.65	0.66	0.66	0.69

Key: COV – Co-efficient of variation.

Table 12
Flexural strength of the NM-blended concretes following exposure to various durations of elevated temperature.

Heating duration (mins)	CC-AC	NM5-AC	NM10-AC	NM15-AC	NM20-AC
0	3.5	3.78	3.99	4.9	4.7
30	3.8	3.8	3.96	4.21	4.37
60	3.01	1.99	2.11	2.13	2.01
90	2.12	0.69	0.78	0.88	0.76
120	0.87	0.15	0.19	0.25	0.2
Mean	2.66	2.08	2.21	2.47	2.41
Standard deviation	1.19	1.70	1.76	2.03	2.05
COV (%)	0.45	0.81	0.80	0.82	0.85
Heating duration (mins)	**CC-WC**	**NM5-WC**	**NM10-WC**	**NM15-WC**	**NM20-WC**
0	3.5	3.78	3.99	4.9	4.7
30	3.78	3.72	3.91	4.14	4.09
60	2.98	1.75	1.99	2	1.98
90	1.09	0.52	0.68	0.79	0.72
120	0.59	0.11	0.18	0.23	0.19
Mean	2.39	1.98	2.15	2.41	2.34
Standard deviation	1.45	1.73	1.77	2.05	2.00
COV (%)	0.61	0.87	0.82	0.85	0.86

Key: COV – Co-efficient of variation.

Table 13
Coefficient of permeability K for the NF-blended concretes.

Sample	Reference value	30 min		60 min		90 min		120 min	
		AC	WC	AC	WC	AC	WC	AC	WC
NF5	5.26e-11	5.26e-11	4.8e-11	5.8e-08	4.3e-08	6.5e-07	4.6e-07	1.1e-06	9.2e-07
NF10	5.08e-11	5.04e-11	4.2e-11	4.9e-08	3.8e-08	6.1e-07	2.7e-07	9.5e-07	7.6e-07
NF15	4.9e-11	4.81e-11	3.9e-11	3.5e-08	2.5e-08	5.4e-07	2.3e-07	8.1e-07	4.6e-07
NF20	4.68e-11	4.6e-11	3.6e-11	2.3e-08	1.1e-08	4.8e-07	2.1e-07	7.8e-07	5.5e-07
NF25	4.53e-11	4.51e-11	3.3e-11	2e-08	1e-08	4.1e-07	1.9e-07	7e-07	4.9e-07

Table 14
Coefficient of permeability K for the NM-blended concretes.

Sample	Reference value	30 min		60 min		90 min		120 min	
		AC	WC	AC	WC	AC	WC	AC	WC
NM5	4.2e-12	4.18e-12	4.1e-12	3.5e-08	3.0e-08	2.7e-07	2.1e-7	2.2e-6	1.5e-6
NM10	3.67e-12	3.72e-12	3.9e-12	3.1e-08	2.9e-08	2.2e-07	1.4e-7	1.9e-06	1.0e-6
NM15	3.12e-12	3.11e-12	3.3e-12	2.9e-08	2.0e-08	1.7e-07	1.0e-7	0.8e-6	0.4e-6
NM20	2.9e-12	2.84e-12	2.7e-12	2.2e-08	0.9e-08	1.5e-07	0.5e-7	0.2e-6	9.8e-5

This was due to the nanomaterials effectively filling the pores present in the mix, making the concrete more compact and denser, thereby restricting water penetration through the capillary pores. However, for temperature-exposed specimens, an increase in the exposure time to high temperatures resulted in greater water permeability. This was attributed to the development of cracks that were observed in the concrete in these cases. These cracks formed a link between the pores in the mix, allowing water to permeate.

The specimens which were water-cooled after heating were shown to possess a higher coefficient of permeability than the corresponding air-cooled specimens; this is likely to be due to the more significant degree of cracking that occurred, especially during the application of cold water to the hot specimen. Owing to the greater number of cracks that developed, this may have had the secondary effect of cracks merging together to form a linkage thus enabling greater water permeability. Irrespective of the mix type, the water-cooled specimens possessed greater coefficients of permeability compared with the corresponding air-cooled specimens in all cases. It is clear that the heating and subsequent cooling of the concrete had an influence on the water permeability of the concrete. In addition, it is observed from the data presented in Table 13 versus that in Table 14, that the type of nanomaterial employed to replace cement did not have a significant effect on the permeability of the concrete.

In summary, the results indicate that the addition of NF and NM to the concrete mix reduced the permeability of the concrete, making it more resistant to water penetration. However, exposure to high temperatures resulted in the development of cracks in the concrete, which increased its permeability.

3.6.2. Rapid chloride penetration test results

The rapid chloride penetration test indirectly measures the permeability and presence of internal pores in the concrete and the test results are generally employed as an indicator of the durability performance of the concrete. The test provides a prediction of the

materials ability to resist chloride ion penetration. The results of the rapid chlorine penetration test are measured in coulombs (equal to an ampere-second, implying that a current of one ampere passed through the concrete specimen in one second would result in one coulomb). A relatively high coulomb value suggests high permeability. The test samples in this programme were subjected to a constant voltage of 60 V for a set period of 6 h and the current passing through the concrete was measured to determine the coulombs.

The results of the rapid chloride penetration tests are presented in Figs. 12 and 13, for the concrete mixes containing NF and NM nanoparticles, respectively. Tables 15 and 16 present the corresponding permeability assessments in accordance with the criteria given in ASTMC 1202:97 [53]. In these tables, the permeability is graded as being either very low (VL), low (L), medium (M) or high (H). From the data presented, it is clear that concrete with a relatively high replacement ratio of nanoparticles, resulted in a relatively low level of penetration of chloride ions through the matrix. This is attributed to the filling of pores in the matrix by nanomaterials, which resulted in a more dense material. This is in agreement with the earlier results from the water penetration test, discussed in the previous sub-section.

The chloride ion penetration was found to be particularly low in the NM-blended mixes compared with the NF-blended concretes; this may be due to the high specific area of the metakaolin. For the specimens exposed to elevated temperatures, the penetration of chloride ions tended to increase for samples that were exposed to longer fire durations; this may be attributed to the relative increase in pore area fraction, which led to a loss in impermeability, and hence durability [41]. When the concrete was subjected to elevated temperature exposure, thermal incompatibility is likely to occur within the matrix, and cracks may develop at the surface and in the core of the concrete. Therefore, in this test, the chloride ions may have penetrated inside the concrete core owing to the presence of these cracks.

3.7. Microstructural analysis

Concrete samples with and without NF or NM nanomaterials, and which were heated for 60 min under a standard fire before being allowed to cool naturally in air, were examined using a scanning electron microscope (SEM) to assess their microstructure. These images given a close view of the cement paste, pore structure and binding relationship between the cement paste and the aggregates, all of which contribute to the development of mechanical strength and durability of concrete. The resulting images are presented in Figs. 14, 15 and 16 for the control concrete, concrete with a replacement ratio of 20% using NF and concrete with a replacement ratio of 15% using NM, respectively. These are selected for demonstration as they were found to be the optimum replacement ratios for each nanomaterial in the mechanical property and durability studies presented earlier in this paper. In all of these figures, (a) presents and an initial image taken at ambient temperature, before heating, and (b) shows the SEM image for the same mix design following 60 min of standard faire exposure and subsequent cooling.

With reference to Fig. 14(a), it is shown that at ambient temperature, the presence of crystalline and amorphous phases is quite visible. In the corresponding images for the mixes with 20% NF (Fig. 15(a)) and 15% NM (Fig. 16(a)), amorphous CSH phases with dense internal structures are observed. Moreover, the concrete blended with NM shows a more dense, compact and perfectly stable microstructure. This corresponds to the greater strength development in this concrete compared with the control concrete. Following exposure to 60 min of elevated temperature, followed by cooling, the residual microstructure of all of the concrete mixes examined in this study changed substantially from the corresponding ambient temperature image. This corresponds with the changes to mechanical properties and durability previously presented.

Following heating and cooling, there was a degradation of the hydrated products in the concrete leading to the formation of larger pores in the internal structure. This was particularly evident for the mixes containing NF and NM, as shown in Figs. 15(b) and 16(b), respectively. In addition, these images show that the cement paste detached from the filler materials thereby creating wider pores and

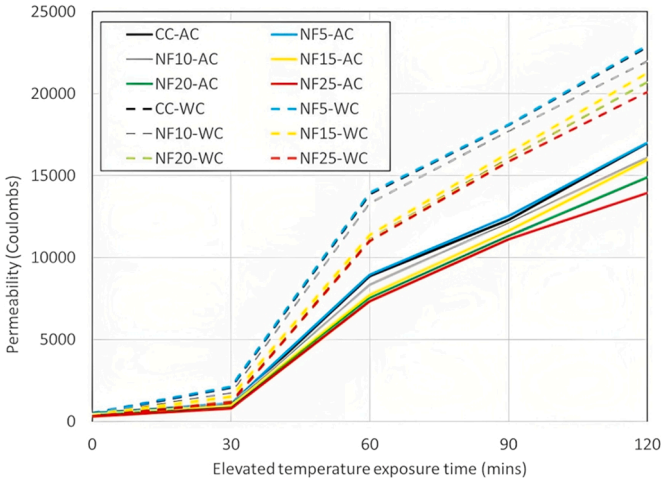

Fig. 12. Residual permeability of NF-blended concrete exposed to elevated temperature and then cooling following the rapid chlorine penetration test.

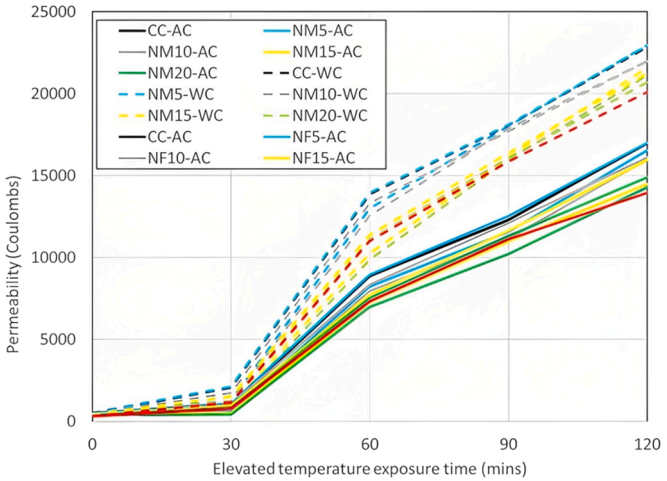

Fig. 13. Residual permeability of NM-blended concrete exposed to elevated temperature and then cooling following the rapid chlorine penetration test.

Table 15
Classification of residual permeability and quality of the concrete with NF nanomaterials in accordance with ASTM C 1202:97 [53].

Sample	30 mins		60 mins		90 mins		120 mins	
	AC	WC	AC	WC	AC	WC	AC	WC
CC	L	M	H	H	H	H	H	H
NF5	L	M	H	H	H	H	H	H
NF10	L	L	H	H	H	H	H	H
NF15	VL	L	H	H	H	H	H	H
NF20	VL	L	H	H	H	H	H	H
NF25	VL	L	H	H	H	H	H	H

Key: VL – Very low, L-Low, H-High, M-Medium.

Table 16
Classification of residual permeability and quality of the concrete with NM nanomaterials in accordance with ASTM C 1202:97 [53].

Sample	30 mins		60 mins		90 mins		120 mins	
	AC	WC	AC	WC	AC	WC	AC	WC
CC	VL	L	H	H	H	H	H	H
NM5	VL	L	H	H	H	H	H	H
NM10	VL	L	H	H	H	H	H	H
NM15	VL	VL	H	H	H	H	H	H
NM20	VL	VL	H	H	H	H	H	H

Key: VL – Very low, L-Low, H-High.

gaps. This internal structure was combined with the degradation of the calcium silicate hydrate (CSH) gel as well as increased cracking. The increase in cracking and pore formation following exposure to heating and cooling was due to a variation in the thermal stresses in the concrete samples both on the surface and internally in the concrete.

3.8. Visual inspection

In this section, the visual appearance of the concrete specimens following the heating and cooling procedure is discussed, in terms of surface crack development and also colour change. The development of cracks is informative in terms of the level of damage in the concrete due to the elevated temperature exposure, whilst the colour change indicates that the different ingredients in the concrete mix, as well as their inter-relationship, has undergone significant change. Concrete which is subjected to fire generally experiences cracking both in the core and also on the surface of the matrix, due to the evaporation of free water molecules in the mix. In previous research, it was shown that the intensity and magnitude of the cracking were found to be negligible when exposed to a temperatures of up to 400 ℃ [54]. When the specimens were subjected to higher temperatures, such as in the current test programme, more surface cracks were visible in all cases.

Fig. 17 present an image for the control case (CC) concrete, without nanomaterials, following exposure to 60 min (925 ℃) and

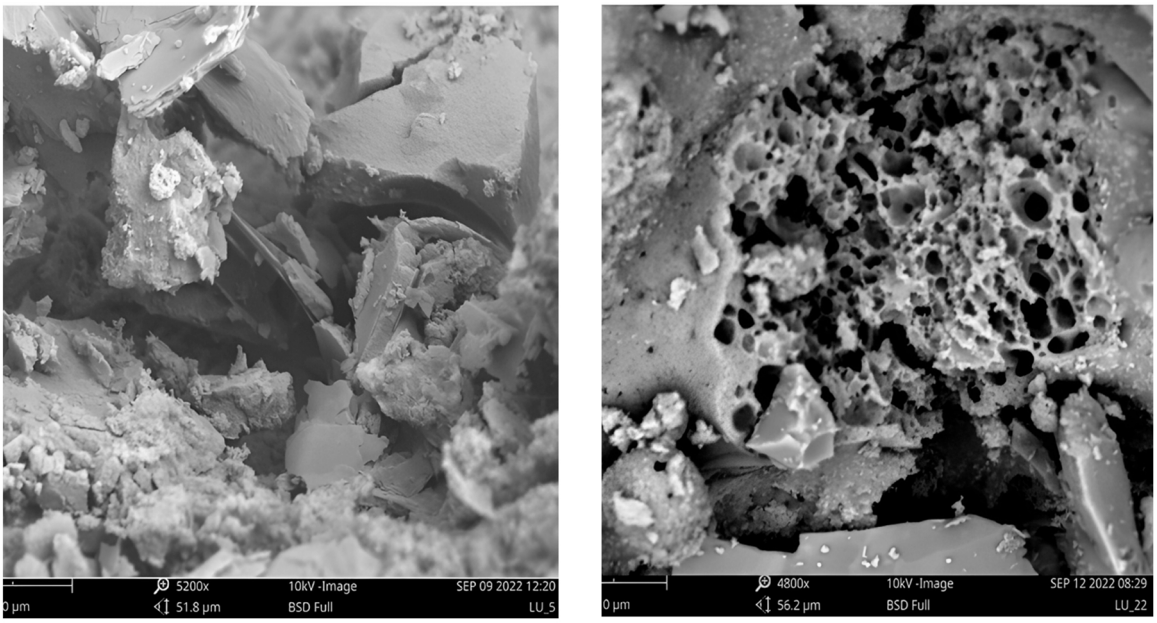

Fig. 14. SEM images from the control concrete at (a) ambient temperature and (b) following exposure to 60 min of standard fire exposure followed by cooling naturally in air.

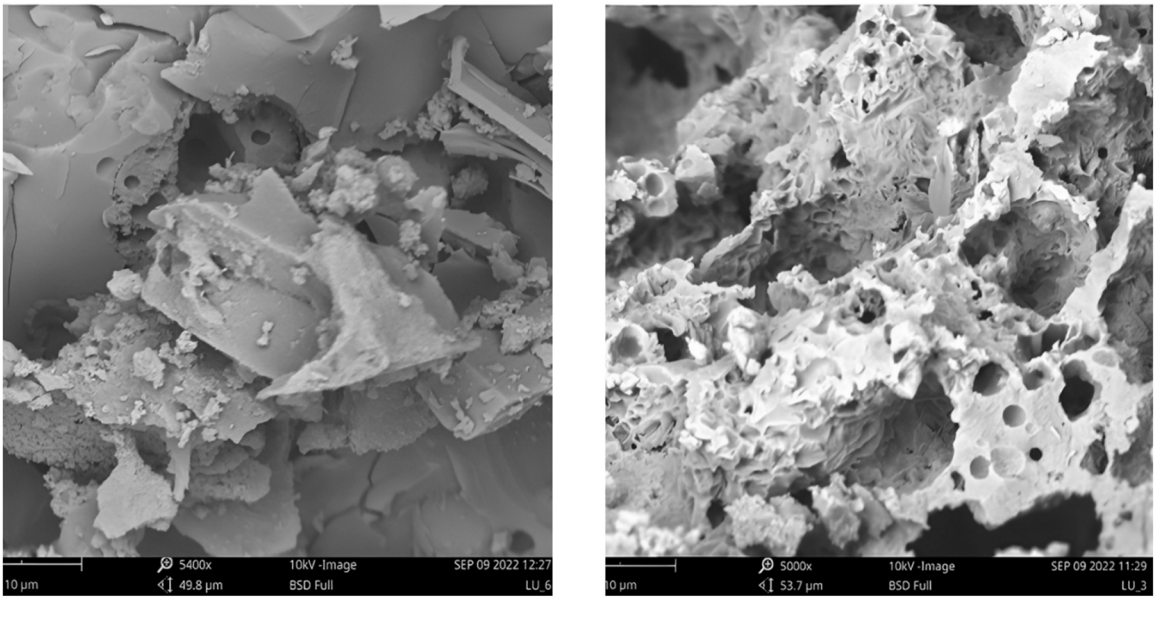

Fig. 15. SEM images from the concrete with 20% of the cement replaced with NF at (a) ambient temperature and (b) following exposure to 60 min of standard fire exposure followed by cooling naturally in air.

120 min (1029 ℃) of elevated temperature, respectively, before being cooled naturally in air. Figs. 18 and 19 present the corresponding images from the surfaces of specimens with 20% and 15% replacement ratio of NF and NM, respectively (these were the optimum replacement ratios for each type of nanomaterial in the mechanical and durability tests described before). Following heating, the control specimens without nanomaterials demonstrated very similar surface behaviour to the concrete specimens containing NM

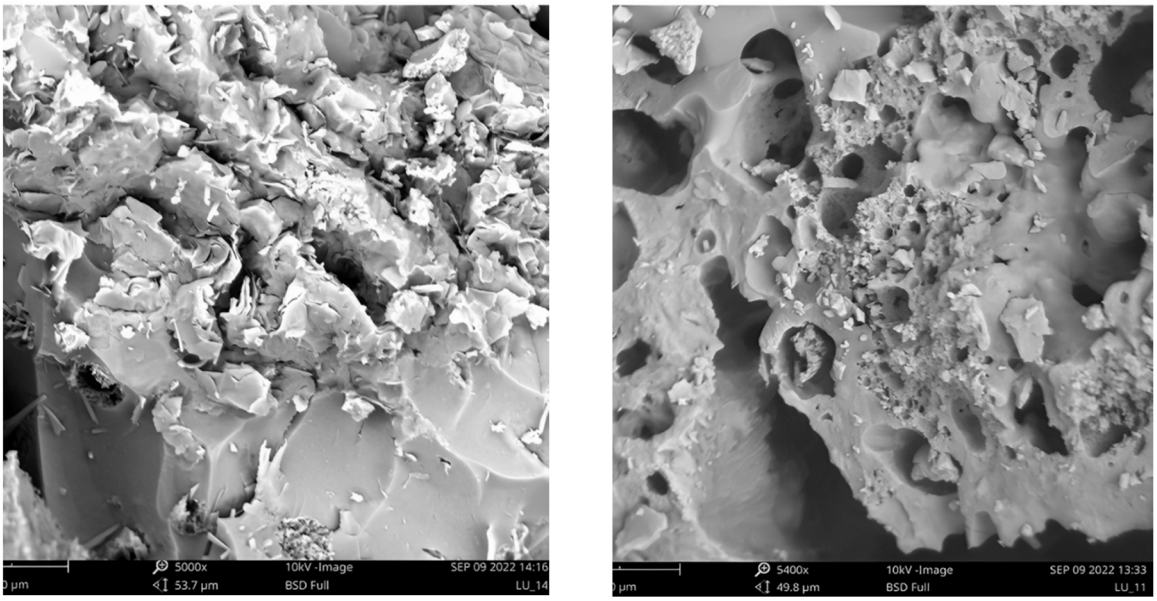

Fig. 16. SEM images from the concrete with 15% of the cement replaced with NF at (a) ambient temperature and (b) following exposure to 60 min of standard fire exposure followed by cooling naturally in air.

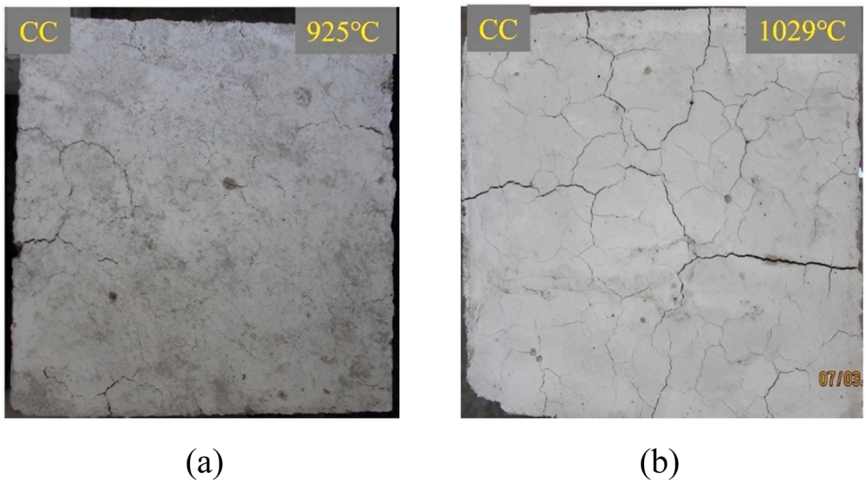

Fig. 17. Surface images of the control case concrete following exposure to (a) 925 ℃ after 60 min and (b) 1029 ℃, after 120 min.

and NF. It is clear that following exposure of up to 925 ℃, there was very little evidence of cracking on the surface of the samples with either NF or NM. On the other hand, after 120 min of standard fire exposure (corresponding to 1029 ℃) followed by cooling, more surface cracks formed in all concrete mixes examined in the current programme. The presence of NM based nanomaterials showed a slight increase in crack density on surface of the concrete but overall the visual response was quite similar.

In terms of the changes of colour of the concrete following exposure to elevated temperature the current test programme, all of the samples examined in this programme (i.e. the control concrete and the concrete blended with various proportions of NF and NM) showed no visible change of colour after 60 min of standard fire (925 ℃). After 120 min of standard fire and subsequent cooling, the control concrete and the mixes with NF as a cement replacement also showed very little colour change. However, for the NM-blended concretes, following exposure to 120 min of standard fire, there was a significant change in the surface colour i.e., from grey to white as shown in Fig. 19. There are a number of possible reasons for this, including the evaporation of water from the concrete at the surface, the escape of free water present in the pores of the matrix and also dehydration of the hydrated phases in the mix [55]. Previous studies have also shown that a reduction in C_4AF in the mix may lead to a colour change [56]. In the temperature range of 600–1000 ℃,

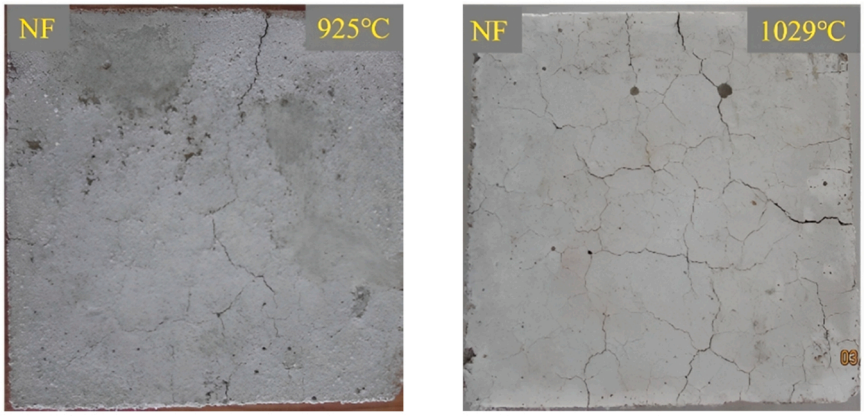

Fig. 18. Surface images of concrete with 20% cement replacement ratio with NF following exposure to (a) 925 ℃ after 60 min and (b) 1029 ℃ after 120 min.

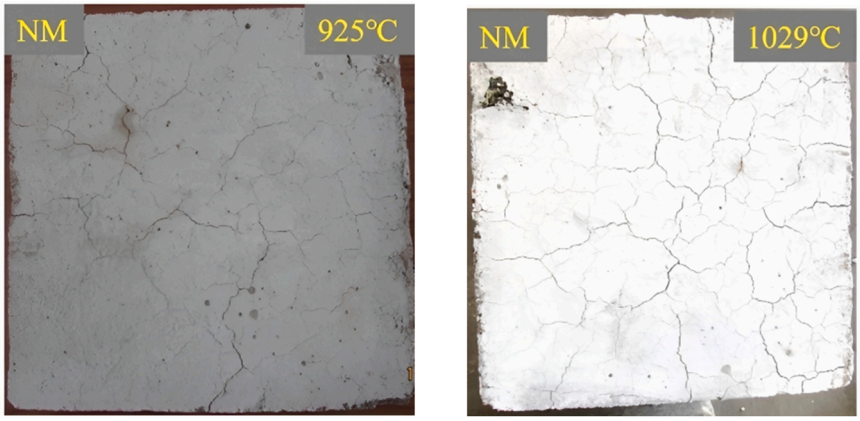

Fig. 19. Surface images of concrete with 15% cement replacement ratio with NM following exposure to (a) 925 ℃ after 60 min and (b) 1029 ℃, after 120 min.

concrete with siliceous aggregates may change colour to whitish-grey due to the carbonation of $CaCO_3$ to lime [57] which may also be factor for the NM-blended concrete, exposed to 120 min of fire.

3.9. Comparison of the results with other published data

A number of researchers have done similar experimental studies to the work presented herein and the most relevant of these are summarised in Table 17. The table includes the dose of nanomaterials employed in the studies, the temperature to which the nanomaterial-blended concrete composites were exposed, whether the nanomaterials were used as an additive or replacement to cement in the concrete mixes, as well as the key outcomes. From the data presented in these works, following observations are deduced:

- The strength of concrete is reduced when it is exposed to high temperatures, and the addition of nanomaterials may not be sufficient to prevent this reduction in strength.
- Nanomaterials may increase the brittleness of concrete following exposure to high temperatures, which could lead to cracking and premature failure.
- Exposure to elevated temperatures can also reduce the durability of concrete, and the addition of nanomaterials may not be sufficient to prevent this reduction in durability.

In the present investigation, it is found that even after exposing to high temperature (temperature $>$ 900 ℃), the nano-fly ash-blended concrete mixes offered superior performance compared with the mixes with nano-metakaolin and it may be advisable to

Table 17
Similar experimental data presented in the literature for the residual properties of various concrete composites following exposure to elevated temperature.

Ref	Nano -material type	Dosage	Temp. (℃)	Substitution/ additive
Sikora et al.[58]				
	Fe_3O_4 and Fe_3O_4/SiO_2	3% and 5%	200–800	Additive
	Key outcomes: Presence of Fe_3O_4 or Fe_3O_4/SiO_2 does not affect flexural strength before and after exposure to fire. Fe_3O_4/SiO_2 nanoparticles present better performance as an admixture by improving the thermal resistance through a reduction in the formation of surface cracks in cement mortars (except after exposure to 800 °C where complete cement structure degradation occurred)			
Polat et al.[13]				
	Halloysite nano-clay, nano-CaO and nano-SiO_2	1%, 3% and 5%	250, 500, 750	Substitution
	Key outcomes: Following exposure to 250 °C and at 500 °C, the compressive strength reduction of the control sample was 18% and 27%, respectively. Following exposure to 750 °C, the compressive strength reduction was lower than for the temperature levels.			
Nalon et al.[59]				
	Multi-walled carbon nanotubes (MWCNT) and carbon-black nanoparticles (CBN)	0.4 – 0.8% and 1.2%, 3%, 6% and 9%	200, 400, 600	Additive
	Key outcomes: Decomposition of nanofillers inside the composite was significant in the samples with 0.4%, 0.8% or 1.2% of MWCNT and 3% or 6% of CBN, following exposure to temperatures higher than 500 °C.			
Sikora et al.[60]				
	Multi-walled carbon nanotubes (MWCNT) and nano-silica	0.125%, 0.25% and 0.5%	300, 450, 600	Substitution
	Key outcomes: MWCNT/NS-incorporated specimens exhibited up to a 20% increase in compressive strength, as compared to the control sample, following exposure to elevated temperature. After exposure to 600 °C, the performance of nearly all sample's containing CNT was worse compared to the control samples. After exposure to such a high temperature, it was found that the CNTs decomposed, resulting in a more porous material compared with a similar mix without CNTs.			
Guler et al.[61]				
	Nano-SiO_2 (NS), nano-TiO_2 (NT), nano-Fe_2O_3 (NF) and nano-Al_2O_3 (NA)	0.5%, 1% and 1.5%	300, 500, 800	Additive
	Key outcomes: The control samples as well as all of the nano-added concrete mixes were observed to maintain their residual compressive strength following exposure to temperatures of up to 300 °C. Following exposure to higher temperatures, there was increasingly significant deterioration of the microstructure of the cement mortars and, consequently, higher strength losses.			
Farzadnia et al.[62]				
	Nano-Al_2O_3	1%, 2% and 3%	100–1000	Substitution
	Key outcomes: The compressive strength of the nano-Al_2O_3-enhanced samples was up to 16% greater than the corresponding residual compressive strength of the control samples. Following exposure to temperatures closer to 1000 °C, the reduction in residual compressive strength was significant for all samples.			
Heikal et al.[63]				
	Nano-silica and nano-silica-GBFS	1% and 4%	200, 400, 650, 850, 950	Substitution
	Key outcomes: It was shown that the residual compressive strength increased following exposure to temperatures of up to 400 °C the nano-silica-blended concrete mixes, whereas it increased following exposure of up to 650 °C for the mixes containing nano-silica-GBFS. Following exposure to higher temperatures (i.e. 850–950 °C), the residual compressive strength was lower than the corresponding original value.			
Present study				
	Nano-fly ash and Nano-metakaolin	5%– 25%	821, 925, 986, 1029	Substitution
	Key outcomes: It is shown that concrete mixes with 20% nano-fly ash which were subjected to temperatures of 925 °C lost 27.8% and 25% of their initial compressive strengths for the air- and water-cooled conditions, respectively. Similarly, concrete with 15% nano-metakaolin experienced a significant strength loss of 53.9% and 52.7% of the corresponding initial values for the air- and water-cooled conditions, respectively, after 60 min (925 °C) of temperature exposure.			

employ nano-fly ash in more fire-prone areas.

4. Conclusions

This paper presents the background and details of an extensive experimental programme, focussed on the post-fire behaviour of concrete containing nanomaterials as a cement replacement material. The motivation to employ cement replacement products is increasing constantly, owing to demands to improve the sustainability credentials of construction products. A large number of different types of cement replacement products have been developed and studied, with nanomaterials attracting much interest in recent times from both the research and practicing engineering communities. This is because they meet both the sustainability requirements, and also improve the mechanical and durability performance of the concrete. However, to date, there is no information available in the public domain regarding their survival and performance following exposure to elevated temperature. This is key information for engineers looking to determine the residual structural capacity of existing concrete structures following a fire, and to potentially save buildings from unnecessary demolition. It is also useful information for emergency workers during and after a building fire, who are likely to be conducting salvage and rescue operations in fire-damaged structures.

The current paper has presented the results and discussion from a large number of experiments which were conducted to determine the post-fire mechanical and durability properties of concrete containing varying amounts of nanomaterials as cement replacement materials. The key findings and observations from these experiments and analysis are given as follows:

- The compressive strength of concrete increases when greater amounts of nano-fly ash (NF) are used as a replacement for cement in the design mix. This is for replacement ratios of up to 20%, which was found in this study to be the optimum value for NF.
- Concrete containing nano-metakaolin (NM) as a cement replacement achieves greater compressive strength compared with traditional concrete and concrete with NF. This is attributed to the high specific area of the NM. Nevertheless, and similarly to NF, the compressive strength of concrete containing NM increases for greater cement replacement ratios, up to an optimum replacement ratio of 15%.
- As expected, for all concrete which is exposed to elevated temperature, the residual mechanical and durability performance reduces for higher levels of temperature exposure and duration. However, the reduction in strength was similar for concretes with nanomaterials compared with regular traditional concrete. The reduction in strength is due to dehydration of the CSH gel phases.
- From the experimental results, it was shown that NM exhibits slightly lower residual strength generally compared with traditional concrete and also the NF blended mix.
- It was found that water/cement ratio, porosity, and specific area are the key influencing parameters affecting the concrete's durability performance following exposure to elevated temperature.
- Due to the relatively high specific area of the NM nanomaterials, the porosity was found to be relatively lower for NM-blended concretes compared with mixes which contain NF; this results in concrete which is relatively compact and dense. Consequently, due to the density and compactness, a relatively high internal pore pressure develops, resulting in greater loss in strength.
- When all of the concretes examined in the current programme were exposed to elevated temperature, the porosity of the mix changed and previously impermeable concrete became more permeable. The relative loss can be greater for concrete containing nanomaterials as a cement replacement, compared with tradition concrete, but this is largely because of their excellent behaviour (and compactness, etc.) at ambient temperature, which degrades in a fire.

It is noteworthy that in the present investigation, the chemical reaction between the binder materials (i.e., the cement and the nanomaterials) after exposure to elevated temperature was not analyzed. This is recommended for future research work. A range of test methods could be employed to study the structural and morphological changes in the gel phases, such as field emission scanning electron microscopy (FSEM), X-Ray diffraction (XRD), thermogravimetric analysis (TGA), Fourier transform infrared spectroscopy (FTIR), or mercury intrusion porosimeter (MIP).

Funding

Fundings are not received for the presented research work.

Declaration of Competing Interest

The authors declare that they have no known competing financial interests or personal relationships that could have appeared to influence the work reported in this paper.

Data Availability

Data will be made available on request.

Acknowledgements

The authors thank the Karunya Institute of Technology and Sciences for providing lab facilities to conduct the research.

References

[1] J. Mañosa, A.M. Gómez-Carrera, A. Svobodova-Sedlackova, A. Maldonado-Alameda, A. Fernández-Jiménez, J.M. Chimenos, Potential reactivity assessment of mechanically activated kaolin as alternative cement precursor, Appl. Clay Sci. 228 (2022), https://doi.org/10.1016/j.clay.2022.106648.
[2] R. Banar, P. Dashti, A. Zolfagharnasab, A.M. Ramezanianpour, A.A. Ramezanianpour, A comprehensive comparison between using silica fume in the forms of water slurry or blended cement in mortar/concrete, J. Build. Eng. 46 (2022), 103802, https://doi.org/10.1016/j.jobe.2021.103802.
[3] C. Liu, M. Zhang, Effect of curing temperature on hydration, microstructure and ionic diffusivity of fly ash blended cement paste: a modelling study, Constr. Build. Mater. 297 (2021), 123834, https://doi.org/10.1016/j.conbuildmat.2021.123834.
[4] R. Li, L. Lei, J. Plank, Impact of metakaolin content and fineness on the behavior of calcined clay blended cements admixed with HPEG PCE superplasticizer, Cem. Concr. Compos. 133 (2022), 104654, https://doi.org/10.1016/j.cemconcomp.2022.104654.
[5] IS 10262, Concrete Mix proportioning-Guidelines, New Delhi, India., 2019.
[6] M.S.M. Norhasri, M.S. Hamidah, A.M. Fadzil, Applications of using nano material in concrete: a review, Constr. Build. Mater. 133 (2017) 91–97, https://doi.org/10.1016/j.conbuildmat.2016.12.005.
[7] J.A. Abdalla, B.S. Thomas, R.A. Hawileh, J. Yang, B.B. Jindal, E. Ariyachandra, Influence of nano-TiO2, nano-Fe2O3, nanoclay and nano-CaCO3 on the properties of cement/geopolymer concrete, Clean. Mater. 4 (2022), https://doi.org/10.1016/j.clema.2022.100061.
[8] D. Praseeda, K.Srinivasa Rao, Durability performance and microstructure analysis of nano engineered blended concrete, Clean. Mater. 6 (2022), 100155, https://doi.org/10.1016/j.clema.2022.100155.
[9] H. Monteiro, B. Moura, N. Soares, Advancements in nano-enabled cement and concrete: innovative properties and environmental implications, J. Build. Eng. 56 (2022), 104736, https://doi.org/10.1016/j.jobe.2022.104736.
[10] M. Amin, M.M. Attia, I.S. Agwa, Y. Elsakhawy, K.A. el-hassan, B.A. Abdelsalam, Effects of sugarcane bagasse ash and nano eggshell powder on high-strength concrete properties, Case Stud. Constr. Mater. 17 (2022), e01528, https://doi.org/10.1016/j.cscm.2022.e01528.

[11] S.A. Mostafa, B.A. Tayeh, I. Almeshal, Investigation the properties of sustainable ultra-high-performance basalt fibre self-compacting concrete incorporating nano agricultural waste under normal and elevated temperatures, Case Stud. Constr. Mater. 17 (2022), e01453, https://doi.org/10.1016/j.cscm.2022.e01453.
[12] G.H. Nalon, J.C.L. Ribeiro, E.N.D. de Araújo, L.G. Pedroti, J.M.F. de Carvalho, R.F. Santos, D.S. de Oliveira, Residual mechanical properties of mortars containing carbon nanomaterials exposed to high temperatures, Constr. Build. Mater. 275 (2021), 122123, https://doi.org/10.1016/j.conbuildmat.2020.122123.
[13] R. Polat, A.W. Qarluq, F. Karagöl, Influence of singular and binary nanomaterials on the physical, mechanical and durability properties of mortars subjected to elevated temperatures and freeze–thaw cycles, Constr. Build. Mater. 295 (2021), 123608, https://doi.org/10.1016/j.conbuildmat.2021.123608.
[14] H.A. Dahish, A.D. Almutairi, Effect of elevated temperatures on the compressive strength of nano-silica and nano-clay modified concretes using response surface methodology, Case Stud. Constr. Mater. 18 (2023), e02032, https://doi.org/10.1016/j.cscm.2023.e02032.
[15] B. Kanagaraj, A. Nammalvar, A.D. Andrushia, B.G.A. Gurupatham, K. Roy, Influence of nano composites on the impact resistance of concrete at elevated temperatures, Fire 6 (2023), https://doi.org/10.3390/fire6040135.
[16] A. Raheem, B. Ikotun, S. Oyebisi, A. Ede, Machine learning algorithms in wood ash-cement-Nano TiO2-based mortar subjected to elevated temperatures, Results Eng. 18 (2023), 101077, https://doi.org/10.1016/j.rineng.2023.101077.
[17] L. Boquera, J.R. Castro, A.L. Pisello, C. Fabiani, A. D'Alessandro, F. Ubertini, L.F. Cabeza, Thermo-mechanical stability of supplementary cementitious materials in cement paste to be incorporated in concrete as thermal energy storage material at high temperatures, J. Energy Storage 54 (2022), 105370, https://doi.org/10.1016/j.est.2022.105370.
[18] S. Alani, M.S. Hassan, A.A. Jaber, I.M. Ali, Effects of elevated temperatures on strength and microstructure of mortar containing nano-calcined montmorillonite clay, Constr. Build. Mater. 263 (2020), 120895, https://doi.org/10.1016/j.conbuildmat.2020.120895.
[19] B. Kanagaraj, N. Anand, A.D. Andrushia, E. Lubloy, Investigation on engineering properties and micro-structure characteristics of low strength and high strength geopolymer composites subjected to standard temperature exposure, Case Stud. Constr. Mater. 17 (2022), e01608, https://doi.org/10.1016/j.cscm.2022.e01608.
[20] A. Sedaghatdoost, K. Behfarnia, Mechanical properties of Portland cement mortar containing multi-walled carbon nanotubes at elevated temperatures, Constr. Build. Mater. 176 (2018) 482–489, https://doi.org/10.1016/j.conbuildmat.2018.05.095.
[21] A. Sedaghatdoost, K. Behfarnia, M. Bayati, The effect of curing period on the residual strength of Portland cement mortar containing MWCNTs at elevated temperature, Constr. Build. Mater. 196 (2019) 144–153, https://doi.org/10.1016/j.conbuildmat.2018.11.119.
[22] S. Hwang, T. Ozbakkaloglu, S.M. Saleem Kazmi, M.J. Munir, Influence of off-spec fly ash and surfactant-coated nano-iron-oxide on the fresh and hardened properties of cement pastes: an exploratory study, J. Build. Eng. 48 (2022), 103976, https://doi.org/10.1016/j.jobe.2021.103976.
[23] J.A. Abdalla, B.S. Thomas, R.A. Hawileh, J. Yang, B.B. Jindal, E. Ariyachandra, Influence of nano-TiO2, nano-Fe2O3, nanoclay and nano-CaCO3 on the properties of cement/geopolymer concrete, Clean. Mater. 4 (2022), https://doi.org/10.1016/j.clema.2022.100061.
[24] F.A. Selim, M.S. Amin, M. Ramadan, M.M. Hazem, Effect of elevated temperature and cooling regimes on the compressive strength, microstructure and radiation attenuation of fly ash–cement composites modified with miscellaneous nanoparticles, Constr. Build. Mater. 258 (2020), 119648, https://doi.org/10.1016/j.conbuildmat.2020.119648.
[25] N. Farzadnia, A.A. Abang Ali, R. Demirboga, M.P. Anwar, Characterization of high strength mortars with nano Titania at elevated temperatures, Constr. Build. Mater. 43 (2013) 469–479, https://doi.org/10.1016/j.conbuildmat.2013.02.044.
[26] B. Kanagaraj, E. Lubloy, N. Anand, V. Hlavicka, T. Kiran, Investigation of physical, chemical, mechanical, and microstructural properties of cement-less concrete – state-of-the-art review, Constr. Build. Mater. 365 (2023), 130020, https://doi.org/10.1016/j.conbuildmat.2022.130020.
[27] R. Samuvel Raj, G. Prince Arulraj, N. Anand, B. Kanagaraj, E. Lubloy, M.Z. Naser, Nanomaterials in geopolymer composites: a review, Dev. Built Environ. 13 (2023), 100114, https://doi.org/10.1016/j.dibe.2022.100114.
[28] H.M. Khater, M. Gharieb, Synergetic effect of nano-silica fume for enhancing physico-mechanical properties and thermal behavior of MK-geopolymer composites, Constr. Build. Mater. 350 (2022), 128879, https://doi.org/10.1016/j.conbuildmat.2022.128879.
[29] M. Bastami, M. Baghbadrani, F. Aslani, Performance of nano-Silica modified high strength concrete at elevated temperatures, Constr. Build. Mater. 68 (2014) 402–408, https://doi.org/10.1016/j.conbuildmat.2014.06.026.
[30] E. Horszczaruk, P. Sikora, K. Cendrowski, E. Mijowska, The effect of elevated temperature on the properties of cement mortars containing nanosilica and heavyweight aggregates, Constr. Build. Mater. 137 (2017) 420–431, https://doi.org/10.1016/j.conbuildmat.2017.02.003.
[31] M. Heikal, M.S. Morsy, I. Aiad, Effect of treatment temperature on the early hydration characteristics of superplasticized silica fume blended cement pastes, Cem. Concr. Res. 35 (2005) 680–687, https://doi.org/10.1016/j.cemconres.2004.06.012.
[32] H. Sardar, R.A. Khushnood, W. Khaliq, H.A. Khan, M.F. Saleem, Influence of pyrolytic waste tire residue on the residual performance of high strength concrete exposed to elevated temperatures, J. Build. Eng. 54 (2022), 104657, https://doi.org/10.1016/j.jobe.2022.104657.
[33] F. He, L. Biolzi, V. Carvelli, Effects of elevated temperature and water re-curing on fracture process of hybrid fiber reinforced concretes, Eng. Fract. Mech. (2022), 108885, https://doi.org/10.1016/j.engfracmech.2022.108885.
[34] J. Guo, H. Yu, H. Ma, Z. Wu, Damage and deterioration characteristics of basic magnesium sulfate cement-coral aggregate concrete exposed to elevated temperature, Eng. Fail. Anal. 137 (2022), 106275, https://doi.org/10.1016/j.engfailanal.2022.106275.
[35] S. Li, J. Zhang, G. Du, Z. Mao, Q. Ma, Z. Luo, Y. Miao, Y. Duan, Properties of concrete with waste glass after exposure to elevated temperatures, J. Build. Eng. 57 (2022), 104822, https://doi.org/10.1016/j.jobe.2022.104822.
[36] M. Shahpari, P. Bamonte, S. Jalali Mosallam, An experimental study on mechanical and thermal properties of structural lightweight concrete using carbon nanotubes (CNTs) and LECA aggregates after exposure to elevated temperature, Constr. Build. Mater. 346 (2022), 128376, https://doi.org/10.1016/j.conbuildmat.2022.128376.
[37] A. Nadeem, S.A. Memon, T.Y. Lo, Evaluation of fly ash and Metakaolin concrete at elevated temperatures through stiffness damage test, Constr. Build. Mater. 38 (2013) 1058–1065, https://doi.org/10.1016/j.conbuildmat.2012.09.034.
[38] M. Amin, Y. Elsakhawy, K. Abu el-hassan, B.A. Abdelsalam, Behavior evaluation of sustainable high strength geopolymer concrete based on fly ash, metakaolin, and slag, Case Stud. Constr. Mater. 16 (2022), e00976, https://doi.org/10.1016/j.cscm.2022.e00976.
[39] Q. Liu, Z. Liu, B. Qian, Y. Xiong, Effect of nano-modified permeable silicone emulsion on the durability of concrete curbstone, Constr. Build. Mater. 324 (2022), 126620, https://doi.org/10.1016/j.conbuildmat.2022.126620.
[40] K. Traven, M. Češnovar, S.D. Škapin, V. Ducman, High temperature resistant fly-ash and metakaolin-based alkali-activated foams, Ceram. Int. 47 (2021) 25105–25120, https://doi.org/10.1016/j.ceramint.2021.05.241.
[41] A. Nadeem, S.A. Memon, T.Y. Lo, The performance of Fly ash and Metakaolin concrete at elevated temperatures, Constr. Build. Mater. 62 (2014) 67–76, https://doi.org/10.1016/j.conbuildmat.2014.02.073.
[42] IS-12269: 2004, Specification for 53 grade ordinary Portland cement, Bur. Indian Stand. (2004) New Delhi,India. https://law.resource.org/pub/in/bis/S03/is.12269.b.1987.pdf.
[43] IS 383, Coarse and fine aggregate for concrete - Specification, New Delhi, India., (2016).
[44] B. Kanagaraj, T. Kiran, A. N, J.S. K. Al Jabri, Development and strength assessment of eco-friendly geopolymer concrete made with natural and recycled aggregates, Constr. Innov. Ahead–p (2022), https://doi.org/10.1108/ci-08-2021-0157.
[45] ASTM C 143, Standard test method for slump of hydraulic-cement concrete, Annu. B. ASTM Stand (2014), https://doi.org/10.1520/C0143.
[46] IS 13311 (Part 1), Method of Non-destructive testing of concret, Part 1: Ultrasonic pulse velocity, Bur. Indian Satandards. (1992) 1–7.
[47] IS 516, Method of Tests for Strength of Concrete -specifications, New Delhi, India., 2004.
[48] IS 5816, Indian standard Splitting tensile strength of concrete- method of test, Bur. Indian Stand (2004) 1–14.
[49] IS:3085, Method of test for Permeability of Cement Mortar and Concrete, Bur. Indian Stand. New Delhi. (2016) 1–12.
[50] ASTM C1202, Standard test method for electrical indication of concrete's ability to resist chloride ion penetration, Am. Soc. Test. Mater. (2012) 1–8, https://doi.org/10.1520/C1202-12.2.

[51] W. Zhou, J. Mo, L. Zeng, S. Xiang, Fracture behavior of polypropylene fiber reinforced concrete modified by rubber powder exposed to elevated temperatures, Constr. Build. Mater. 346 (2022), 128439, https://doi.org/10.1016/j.conbuildmat.2022.128439.
[52] M. Ealiyas Mathews, T. Kiran, N. Anand, E. Lubloy, M.Z. Naser, G. Prince Arulraj, Effect of protective coating on axial resistance and residual capacity of self-compacting concrete columns exposed to standard fire, Eng. Struct. 264 (2022), 114444, https://doi.org/10.1016/j.engstruct.2022.114444.
[53] ASTM C1202, Standard test method for electrical indication of concrete's ability to resist chloride ion penetration, Am. Soc. Test. Mater. (2012) 1–8.
[54] M. Esfahani, M. Hoseinzade, M. Shakiba, F. Arbab, M. Yekrangnia, G. Pachideh, Experimental investigation of residual flexural capacity of damaged reinforced concrete beams exposed to elevated temperatures, Eng. Struct. 240 (2021), 112388, https://doi.org/10.1016/j.engstruct.2021.112388.
[55] M.E. Mathews, A. N, D.A. A, T. Kiran, K. Al-Jabri, Flexural behavior of fire damaged self-compacting concrete beams strengthened with fiber reinforced polymer (FRP) wrapping, J. Struct. Fire Eng. 12 (2021) 486–509, https://doi.org/10.1108/JSFE-02-2021-0007.
[56] H. Sanaei Ataabadi, A. Sedaghatdoost, H. Rahmani, A. Zare, Microstructural characterization and mechanical properties of lightweight polymer concrete exposed to elevated temperatures, Constr. Build. Mater. 311 (2021), 125293, https://doi.org/10.1016/j.conbuildmat.2021.125293.
[57] S.S. Raza, L.A. Qureshi, Effect of carbon fiber on mechanical properties of reactive powder concrete exposed to elevated temperatures, J. Build. Eng. 42 (2021), https://doi.org/10.1016/j.jobe.2021.102503.
[58] P. Sikora, K. Cendrowski, E. Horszczaruk, E. Mijowska, The effects of Fe3O4 and Fe3O4/SiO2 nanoparticles on the mechanical properties of cement mortars exposed to elevated temperatures, Constr. Build. Mater. 182 (2018) 441–450, https://doi.org/10.1016/j.conbuildmat.2018.06.133.
[59] G.H. Nalon, J.C. Lopes Ribeiro, L.G. Pedroti, E.N. Duarte de Araújo, J.M. Franco de Carvalho, G.E. Soares de Lima, L. de Moura Guimarães, Residual piezoresistive properties of mortars containing carbon nanomaterials exposed to high temperatures, Cem. Concr. Compos. 121 (2021), https://doi.org/10.1016/j.cemconcomp.2021.104104.
[60] P. Sikora, M. Abd Elrahman, S.Y. Chung, K. Cendrowski, E. Mijowska, D. Stephan, Mechanical and microstructural properties of cement pastes containing carbon nanotubes and carbon nanotube-silica core-shell structures, exposed to elevated temperature, Cem. Concr. Compos. 95 (2019) 193–204, https://doi.org/10.1016/j.cemconcomp.2018.11.006.
[61] S. Guler, Z.F. Türkmenoğlu, A. Ashour, Performance of single and hybrid nanoparticles added concrete at ambient and elevated temperatures, Constr. Build. Mater. 250 (2020) 27–30, https://doi.org/10.1016/j.conbuildmat.2020.118847.
[62] N. Farzadnia, A.A. Abang Ali, R. Demirboga, Characterization of high strength mortars with nano alumina at elevated temperatures, Cem. Concr. Res. 54 (2013) 43–54, https://doi.org/10.1016/j.cemconres.2013.08.003.
[63] M. Heikal, O.K. Al-Duaij, N.S. Ibrahim, Microstructure of composite cements containing blast-furnace slag and silica nano-particles subjected to elevated thermally treatment temperature, Constr. Build. Mater. 93 (2015) 1067–1077, https://doi.org/10.1016/j.conbuildmat.2015.05.042.